Available online at www.sciencedirect.com

ScienceDirect

Geochimica et Cosmochimica Acta 186 (2016) 13–31

Geochimica et Cosmochimica Acta

www.elsevier.com/locate/gca

Spatial heterogeneity of sources of branched tetraethers in shelf systems: The geochemistry of tetraethers in the Berau River delta (Kalimantan, Indonesia)

Jaap S. Sinninghe Damsté *

NIOZ Royal Netherlands Institute for Sea Research, Department of Marine Microbiology and Biogeochemistry, and Utrecht University, P.O. Box 59, 1790 AB Den Burg, Texel, The Netherlands
Utrecht University, Faculty of Geosciences, P.O. Box 80.021, 3508 TA Utrecht, The Netherlands

Received 5 February 2016; accepted in revised form 18 April 2016; available online 29 April 2016

Abstract

The bulk organic matter composition (total organic carbon (TOC) content and $\delta^{13}C_{TOC}$) and composition of isoprenoid and branched glycerol dialkyl glycerol tetraethers (GDGT) in surface sediments from 43 stations in the Berau River delta (east Kalimantan, Indonesia), including two coast-shelf transects and stations within the river mouth, were examined to reveal the spatial heterogeneity in these parameters in order to assess the impact of a tropical river loaded with suspended matter on the sedimentary organic matter in the shelf system. The high-resolution study showed that, despite the extensive transport of eroded soil material by the river to the sea, terrestrial organic matter and brGDGTs are only deposited on a relatively small part of the shelf. The concentrations of brGDGTs are highest (up to 120 μg g^{-1} TOC) in sediments deposited in and close to the mouth of the Berau River and their distribution indicates that they represent a mixture of soil-derived and river in-situ produced brGDGTs. Crenarchaeol concentrations reach 700 μg g^{-1} TOC in sediments deposited on the outer shelf due to Thaumarchaeotal production in shelf waters. This results in a strong gradient (0.93–0.03) in the BIT index, with high values in the river mouth and low values on the shelf. The decline in the BIT index is caused by both decreasing concentrations of the brGDGTs and increasing concentrations of crenarchaeol. The BIT index shows a highly significant but non-linear relationship with $\delta^{13}C_{TOC}$. On the shelf, in the area not under the direct influence of the Berau River, cyclic brGDGTs become relatively dominant, most probably due to in-situ production in the alkaline pore waters of the surface sediments. The spatial heterogeneity of sources of brGDGTs on the Berau shelf complicates the use of brGDGTs as temperature proxies. Application of the global soil calibration to sedimentary mixtures of brGDGTs in the river-influenced area of the shelf results in a severe underestimation of mean annual air temperature (MAT) by 6 °C. This is due to the mixed origin of the brGDGTs, which are not only derived from soil erosion but, likely, also from riverine production, as has been observed for other river systems.

Comparison of the Berau shelf other shelf systems indicates that in-situ production of brGDGTs in shelf sediments is a widespread phenomenon that is especially pronounced at water depths of ca. 50–300 m. It is hypothesized that this is so because benthic in-situ production of heterotrophic brGDGT-producing bacteria is fueled by the higher delivery of fresh organic matter to these sediments as the consequence of higher primary productivity in shelf waters and a decreased mineralization due to the relatively short settling times of particles on the shelf. For palaeoclimatic studies of marine shelf sediments the application of brGDGTs as proxies is severely complicated by the heterogeneity of sources of brGDGTs. Comparison of

* Address: NIOZ Royal Netherlands Institute for Sea Research, Department of Marine Microbiology and Biogeochemistry, and Utrecht University, P.O. Box 59, 1790 AB Den Burg, Texel, The Netherlands.
E-mail address: jaap.damste@nioz.nl.

http://dx.doi.org/10.1016/j.gca.2016.04.033
0016-7037/© 2016 The Author. Published by Elsevier Ltd.
This is an open access article under the CC BY license (http://creativecommons.org/licenses/by/4.0/).

the brGDGT composition of soils with those of shelf sediments may assist in deciding if sedimentary brGDGTs are predominantly derived from soil erosion. Several methods to do so are discussed.
© 2016 The Author. Published by Elsevier Ltd. This is an open access article under the CC BY license (http://creativecommons.org/licenses/by/4.0/).

Keywords: GDGT; Tetraether; Branched GDGT; Isoprenoid GDGT; BIT index; Temperature reconstruction; Shelf sea; Estuary; Soil; Riverine organic matter; Terrestrial organic matter; Surface sediments; Berau River; Svalbard fjord; South China Sea; Portuguese margin; Kara Sea

1. INTRODUCTION

Glycerol dialkyl glycerol tetraethers (GDGTs) are organic compounds occurring in membranes of archaea and bacteria and have recently raised substantial interest due to their potential as biomarkers and proxies (see Schouten et al., 2013b for a review). Specific isoprenoid GDGTs are used as tracers for (living) archaeal cells in oceans, lakes and the deep biosphere. For example, the isoprenoid GDGT crenarchaeol is specific for nitrifying archaea belonging to the Thaumarchaeota (Sinninghe Damsté et al., 2002) and ^{13}C-depleted isoprenoid GDGTs with one or two cyclopentane moieties are characteristic for archaea involved in the anaerobic oxidation of methane (Pancost et al., 2001). In contrast, the exact biological sources of branched GDGTs (brGDGTs) remain enigmatic, although there are indications that they may be sourced by Acidobacteria (Sinninghe Damsté et al., 2011, 2014).

Several proxies based on GDGTs have been developed such as the TEX_{86} for sea surface temperature reconstruction and the BIT index for soil organic matter input (Schouten et al., 2013b). One of the interesting applications for palaeoclimatology is the use of brGDGTs in shallow marine sediments to reconstruct continental climate (Weijers et al., 2007a) based on the premise that brGDGTs produced in soil are brought by rivers to coastal regions. Since the distribution of the brGDGTs reflects the temperature and pH of the soil at the time of the production of the bacterial membranes, expressed in the MBT/CBT indices (Weijers et al., 2007b), the fossilized brGDGTs in coastal marine sediments may provide a record of past variations in the temperature of the catchment of the river system, enabling continental climate reconstructions. By reconstructing both continental and sea temperature using one marine core inferences about the contrast in temperature between sea and land may be made and its impact on the hydrology (e.g., Weijers et al., 2007a). In the last years, however, various complications with this approach, such as the provenance of soil-derived brGDGTs (Bendle et al., 2010) and potential in-situ production in the river (Zell et al., 2013a,b; De Jonge et al., 2014b), the oxic (Zell et al., 2014a,b; De Jonge et al., 2015) and anoxic (Liu et al., 2014; Xie et al., 2014) marine water column, and in marine sediments (e.g. Peterse et al., 2009a; Zhu et al., 2011), have been recognized.

Here, GDGT proxies in the delta of a river system draining a tropical rain forest are evaluated. The Berau River delta is located in NE Kalimantan (Indonesia), where the river enters into the Sulawesi Sea. The delta has an area of ca. 800 km^2, varies in depth from a few to 100 m, and is shielded from the open ocean by coral reefs, resulting in calm waters. We analyzed surface sediments from 43 stations (Fig. 1) for bulk parameters (TOC content, $\delta^{13}C_{TOC}$) and GDGTs using LC-MS techniques enabling the separation of the 5- and 6-methyl brGDGTs (cf. De Jonge et al., 2014a; Hopmans et al., 2016). These results are discussed in comparison with data from other river delta systems and global soils to evaluate the consequences for the application of GDGT proxies in palaeoclimate studies.

2. MATERIALS AND METHODS

2.1. Setting

The Berau shelf (Fig. 1) is approximately 50 km wide and separated from the Makassar Strait by a steep slope. The steep edge of the shelf is topped by extensive barrier reefs in the north (Pulau Panjang to Pulau Semama complex) and south (Karang Besar complex), but in the central part the shelf break is at 100–120 m water depth (Fig. 1b). A large river, the Berau River, discharges over the shelf area. Yearly precipitation in the Berau region is ca. 2900 mm yr^{-1} with only moderate changes in monthly precipitation. The Berau River discharges a plume extending up to 15 km over the shelf, but in the wet season it might reach as far as the barrier islands in the North, about 30 km off shore (Renema, 2006). The catchment of the river is ca. 100 km^2 and consists for the major part of rainforest, although forest clearing in recent years is affecting this, resulting, in combination with the high rainfall, to a high suspended matter load in the river (2 Mt y^{-1}; Buschman et al., 2012) and high sedimentation rates in the delta (up to 3 cm y^{-1}).

2.2. Sampling

Surface sediments (usually 0–1 cm, in other cases 1–2 cm) from 26 stations (see Table 1) in the Berau River delta on two coast-shelf transects (Fig. 1; Transects A and B) were retrieved by sub-sampling of box cores obtained during a cruise of the R/V Geomarin I in July 2003. Surface sediments (0–5 cm) from 17 stations closer to the river mouth (Fig. 1) were collected in April 2007 using a Smith-McIntyre grab sampler as described by Booij et al. (2012).

During the 2007 expedition also a 100 cm long sediment core was obtained at station 11B by a scuba diver. Nine selected 3 cm-slices of this core were also studied. Appreciable excess ^{210}Pb activity (Table 2) was detected over the entire depth of the measured profile, indicating that there is a layer of at least 1 m of relatively recent sediment of 100–150 years old present at the coring location. In the upper 50 cm of the core no downcore decrease in ^{210}Pb

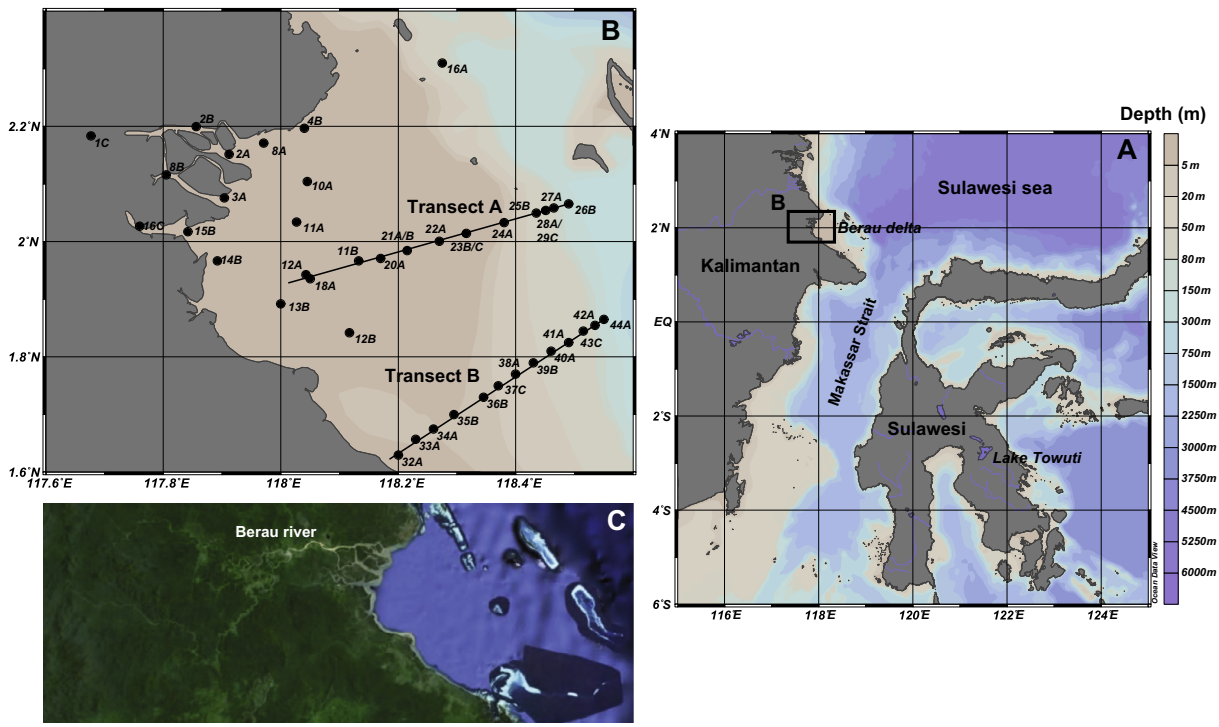

Fig. 1. (A) Location of the Berau River and its delta in eastern Kalimantan (Indonesia). (B) The locations of the stations in the Berau delta. The two coast-shelf break transects (Tansect A, length 51 km and Tansect B, length 47 km) are indicated. For both maps water depth (in m) is indicated by the scale bar at the right. Lake Towit in Sulawesi is indicated since brGDGT distributions from this lake system have been reported. (C) Satellite image (Google Earth) of the Berau River watershed and its delta with the shallow barrier reefs.

activity was observed, indicating thorough mixing of the upper 50 cm. Below this depth ^{210}Pb activity showed a smooth exponential decrease, probably indicating radioactive decay of ^{210}Pb in progressively older sediment layers.

2.3. Bulk measurements

Carbonate was removed by treating sediment samples at 50 °C with 2 mol L^{-1} HCl overnight. Samples were subsequently analyzed with a Thermo Finnigan Flash 1112 series Elemental Analyzer interfaced with a Thermo Finnigan Delta^{Plus} mass spectrometer. The TOC content is expressed as the weight percentage of dried sediment (wt.%). The $\delta^{13}C_{TOC}$ values are reported in the standard delta notation relative to Vienna Pee Dee Belemnite standard (VPDB). For calibration an acetanilide standard with a known TOC content and a $\delta^{13}C$ value calibrated against NBS-22 oil was used. The analyses were determined at least in duplicate and the analytical error was typically <0.1 wt.% for the TOC content and <0.1 ‰ for the $\delta^{13}C_{TOC}$.

2.4. Lipid extraction and GDGT analysis

Homogenized sediments (1–2 g) were freeze dried and subsequently extracted using accelerated solvent extraction (ASE; Dionex) with a 9:1 (v/v) mixture of dichloromethane and methanol (100 °C, 3x). An internal GDGT standard (Huguet et al., 2006) was added to the extract. The extract was subsequently separated on a small Al_2O_3 column into separate fractions (see Hopmans et al., 2004). The polar fraction was analyzed for GDGTs using high performance liquid chromatography-atmospheric pressure chemical ionization-mass spectrometry (HPLC-APCI-MS) using a method enabling the separation of 5- and 6-methyl brGDGTs (Hopmans et al., 2016). Detection was via selected ion monitoring (SIM; Schouten et al., 2007) using *m/z* 744 for the internal standard, *m/z* 1302, 1300, 1298, 1296, and 1292 for isoprenoid GDGTs including crenarchaeol and *m/z* 1050, 1048, 1046, 1036, 1034, 1032, 1022, 1020 and 1018 for brGDGTs. Agilent Chemstation software was used to integrate peak areas in the mass chromatograms of the $[M+H]^+$ ions. Concentrations of GDGTs (normalized on TOC content) were calculated using the known concentration of the internal standard and assuming a similar mass spectrometric response for the isoprenoid and branched GDGTs measured. A slightly higher response factor of branched GDGTs compared to crenarchaeol has been reported for most of the MS systems used in determining the BIT index (Schouten et al., 2013a), and so the reported BIT index values are likely slightly too high. However, the BIT index values will predominantly be used for determining trends in the dataset.

2.5. Calculation of GDGT-based proxies

The BIT index was calculated according to Hopmans et al. (2004). The inclusion of 6-methyl brGDGTs (De Jonge et al., 2013) is indicated explicitly:

$$BIT = [(Ia) + (IIa) + (IIIa) + (IIa') + (IIIa')]/[(Ia) + (IIa) + (IIIa) + (IIa') + (IIIa') + (IV)] \quad (1)$$

Table 1
Location of research stations for surface sediment sampling in the Berau delta, some general organic matter properties, and the concentration of crenarchaeol, summed brGDGTs, and values for the BIT index and TEX_{86}.

Station	Latitude (°E)	Longitude (°N)	Water depth (m)	TOC (%)	$\delta^{13}C_{TOC}$ (‰)	Crenarchaeol (μg g^{-1} TOC)	brGDGTs (μg g^{-1} TOC)	BIT index	TEX_{86}
1C	117.677	2.184	2	0.94	−30.0	8	117	0.93	0.66
2A	117.912	2.152	4	0.97	−29.4	46	94	0.63	0.68
2B	117.856	2.200	2	2.22	−29.0	81	104	0.52	0.72
3A	117.904	2.076	4	2.09	−29.7	38	86	0.66	0.69
4B	118.040	2.197	5	0.16	−25.8	183	114	0.32	0.68
8A	117.971	2.171	1	2.79	−28.3	71	109	0.57	0.67
8B	117.805	2.116	5	1.52	−29.3	26	104	0.78	0.69
10A	118.045	2.104	13	2.08	−28.6	81	86	0.47	0.65
11A	118.027	2.034	4	2.08	−29.3	35	61	0.60	0.66
11B	118.133	1.967	30	2.24	−27.5	190	57	0.19	0.61
12A	118.043	1.943	20	2.26	−28.4	102	69	0.35	0.62
12B	118.117	1.842	25	1.92	−26.7	245	59	0.16	0.60
13B	118.000	1.892	4	2.04	−27.8	66	42	0.34	0.65
14B	117.892	1.967	6	2.74	−28.2	116	67	0.32	0.61
15B	117.842	2.017	6	2.61	−29.2	93	91	0.45	0.67
16A	118.275	2.310	132	0.18	−20.0	393	35	0.05	0.68
16C	117.760	2.027	12	8.23	−29.6	23	46	0.64	0.72
18A	118.050	1.936	7	2.18	−28.3	92	67	0.38	0.62
20A	118.170	1.971	35	1.43	−24.4	485	50	0.07	0.64
21A	118.215	1.985	50	0.98	−22.2	558	42	0.05	0.64
21B	118.215	1.985	50	0.74	−22.3	669	51	0.05	0.64
22A	118.270	2.001	47	0.71	−21.3	671	45	0.04	0.66
23B	118.314	2.014	67	0.52	−21.0	584	38	0.04	0.69
23C	118.316	2.015	67	0.57	−20.7	516	27	0.03	0.69
24A	118.380	2.033	67	0.08	−20.8	134	16	0.05	0.72
25B	118.435	2.050	38	0.03	−20.7	665	69	0.04	0.71
26B	118.490	2.066	195	0.04	−21.5	199	14	0.05	0.68
27A	118.465	2.058	91	0.09	−20.3	170	15	0.04	0.72
28A	118.449	2.054	58	0.08	−20.3	301	20	0.03	0.71
29C	118.451	2.054	50	0.06	−20.6	269	22	0.03	0.71
32A	118.200	1.630	6	1.27	−23.4	396	51	0.09	0.59
33A	118.230	1.657	26	0.98	−22.3	529	44	0.05	0.62
34A	118.260	1.675	29	0.94	−22.0	652	44	0.04	0.63
35B	118.295	1.700	39	0.54	−21.9	681	44	0.04	0.65
36B	118.345	1.730	52	0.45	−21.6	628	41	0.04	0.66
37C	118.370	1.750	51	0.44	−21.8	582	34	0.03	0.66
38A	118.400	1.770	56	0.42	−22.0	688	37	0.03	0.66
39B	118.430	1.790	45	0.44	−22.7	509	32	0.04	0.67
40A	118.460	1.810	55	0.41	−22.7	461	31	0.04	0.68
41A	118.490	1.825	58	0.45	−23.4	346	28	0.05	0.68
42A	118.515	1.845	53	0.23	−23.9	594	44	0.05	0.67
43C	118.535	1.855	71	0.21	−24.5	371	42	0.07	0.68
44A	118.550	1.865	109	0.07	−22.4	331	80	0.14	0.69

Table 2
Bulk and GDGT properties of sediment layers of the core from Station 11B in the Berau delta.

Depth (cm)	^{210}Pb(tot) (mBq g^{-1})	TOC (%)	$\delta^{13}C_{TOC}$ (‰)	Crenarchaeol (μg g^{-1} TOC)	brGDGTs (μg g^{-1} TOC)	BIT index	TEX_{86}	$\#rings_{tetra}$	%tetra
0–2	83.7	2.13	−27.6	226	44	0.135	0.584	0.301	81.4
5–8	85.4	2.53	−28.6	177	37	0.142	0.582	0.295	81.8
26–29	90.6	2.14	−27.6	198	41	0.141	0.587	0.305	80.6
35–38	88.7	2.06	−27.6	205	42	0.141	0.587	0.301	80.7
47–50	90.0	2.21	−27.8	210	40	0.131	0.591	0.301	80.7
59–62	78.7	1.89	−27.6	283	57	0.140	0.599	0.285	80.8
71–74	62.0	1.78	−27.5	192	39	0.140	0.585	0.281	80.5
83–86	53.0	1.81	−27.7	203	40	0.137	0.590	0.282	80.8
95–98	48.0	2.10	−27.9	204	38	0.131	0.584	0.289	80.5

The roman numerals in brackets refer to the concentrations of GDGTs whose structures are shown in the Appendix. Ia is the basic tetramethyl brGDGT, IIa and IIIa are 5-methyl brGDGTs, IIa′ and IIIa′ are 6-methyl brGDGTs, and IV is the isoprenoid GDGT (iGDGT) crenarchaeol, a GDGT specific for Thaumarchaeota (Sinninghe Damsté et al., 2002).

To evaluate brGDGT distributions various ratios were calculated based on the fractional abundances (indicated by using square brackets) of the brGDGTs.

$$\%\text{tetra} = \Sigma[\text{tetramethylated brGDGTs}] = [\text{Ia}] + [\text{Ib}] + [\text{Ic}] \quad (2)$$

$$\%\text{penta} = \Sigma[\text{pentamethylated brGDGTs}] = [\text{IIa}] + [\text{IIb}] + [\text{IIc}] + [\text{IIa}'] + [\text{IIb}'] + [\text{IIc}'] \quad (3)$$

$$\%\text{penta} = \Sigma[\text{hexamethylated brGDGTs}] = [\text{IIIa}] + [\text{IIIb}] + [\text{IIIc}] + [\text{IIIa}'] + [\text{IIIb}'] + [\text{IIIc}'] \quad (4)$$

The weighted average number of cyclopentane moieties was calculated for the tetra- and pentamethylated brGDGTs as follows:

$$\#\text{rings}_{\text{tetra}} = ([\text{Ib}] + 2^*[\text{Ic}])/([\text{Ia}] + [\text{Ib}] + [\text{Ic}]) \quad (5)$$

$$\#\text{rings}_{\text{penta 5Me}} = ([\text{IIb}] + 2^*[\text{IIc}])/([\text{IIa}] + [\text{IIb}] + [\text{IIc}]) \quad (6)$$

$$\#\text{rings}_{\text{penta 6Me}} = ([\text{IIb}'] + 2^*[\text{IIc}'])/([\text{IIa}'] + [\text{IIb}'] + [\text{IIc}']) \quad (7)$$

The isomer ratio (IR) represents the fractional abundance of the penta- and hexamethylated 6-Me brGDGTs vs. the total of penta- and hexamethylated brGDGTs (modified after De Jonge et al., 2014a) and was separately calculated for penta- and hexamethylated brGDGTs:

$$\text{IR}_{\text{penta}} = ([\text{IIa}'] + [\text{IIb}'] + [\text{IIc}'])/\Sigma[\text{pentamethylated brGDGTs}] \quad (8)$$

$$\text{IR}_{\text{hexa}} = ([\text{IIIa}'] + [\text{IIIb}'] + [\text{IIIc}'])/\Sigma[\text{hexamethylated brGDGTs}]. \quad (9)$$

2.6. Data processing

For constructing surface plots the data was plotted using Ocean Data View (odv.awi.de) software using DIVA gridding. PCA was performed on the fractional abundances of all brGDGTs (excepting IIIb, IIIc, IIIb′, and IIIc′, which all had a fractional abundance < 1% of total brGDGTs) using Sigma Plot© version 13.0.

3. RESULTS

3.1. Bulk parameters

The TOC content of the surface sediments varies from 0.05 to 8.2 wt.% and the $\delta^{13}C_{TOC}$ varied from −30.0‰ to −20.3‰ (Table 1). The surface plots for TOC content and $\delta^{13}C_{TOC}$ (Fig. 2A and B) reveal that in and close to the river mouth the TOC content of the surface sediments is high and $\delta^{13}C_{TOC}$ values are most negative, while low TOC sediments with more positive stable carbon isotope values are found along the stations of the two transects further from the coast seawards and station 16A (Fig. 1). In both parameters a gradual transition from the river mouth to the shelf is observed.

In the sediment core from station 11B the TOC content varied from 1.8 to 2.5 wt.% and $\delta^{13}C_{TOC}$ varied from −27.5‰ to −28.6‰ (Table 2).

3.2. GDGTs in surface sediments

Crenarchaeol (IV) contributes on average almost 70% of the isoprenoid GDGTs with concentrations varying between 8 and 690 μg g TOC^{-1} (Table 1). The surface plot of the crenarchaeol concentration shows that it maximizes on the shelf in waters between 25 and 70 m (Fig. 2C). The regioisomer of crenarchaeol is more abundant in surface sediments at stations with increased water depth; it contributes 1–6% to the total sum of crenarchaeol and this value shows a significant correlation with water depth ($r^2 = 0.89$) with one outlier, which is the most inland station (1C). Surface sediments from inland river stations also show deviations in the abundance of GDGT-0, which goes up from average fractional abundances of ca. 10% to almost 60% in station 1C, and GDGT-2 (VII), which increase from ca. 6% on the shelf to 8–15% in the inland river stations. TEX_{86} values vary from 0.59 to 0.72 (Table 1), corresponding to reconstructed sea water temperatures of 24–29 °C using the TEX_{86}^{H} calibration of Kim et al. (2010a), with slightly increasing values towards the outer shelf.

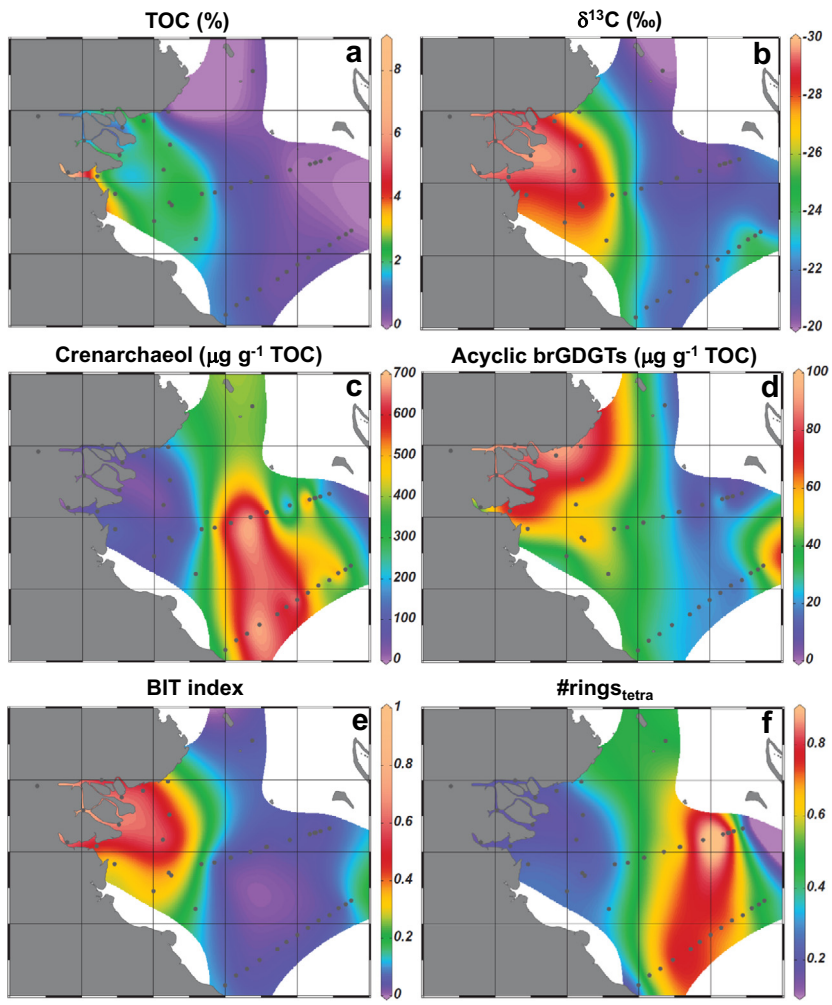

Fig. 2. Isosurface plots for the Berau delta surface sediments of (A) TOC content (%), (B) $\delta^{13}C_{TOC}$ (‰), (C) crenarchaeol concentration (µg g TOC^{-1}), (D) summed concentration of acyclic brGDGT (µg g TOC^{-1}), (E) BIT index, and (F) $\#rings_{tetra}$.

The summed concentration of brGDGTs varies from 10 to 120 µg g TOC^{-1} (Table 1), with higher concentrations in the surface sediments within or close to the mouth of the river. The concentrations of the acyclic[1] brGDGTs, which have been used as indicators of terrestrial organic matter transport (Hopmans et al., 2004), show relatively high concentrations (i.e. >60 µg g TOC^{-1}) at stations close to the river mouth and much lower concentrations in shelf stations (Fig. 2D). Together with an opposite trend in crenarchaeol concentration (Fig. 2C), this results in high values of the BIT index in stations in or close to the river mouth and low (<0.1) values on the shelf at water depths > 30 m (Fig. 2E).

The distribution of the brGDGTs is dominated by tetramethylated brGDGTs (61–82%; see Table 3 for the individual fractional abundances) and the novel 6-methyl brGDGTs comprise 10–25%, less than in the average soil (De Jonge et al., 2014a). A marked change is observed in the distribution of brGDGTs on the transect from river mouth to shelf break. Principal component analysis (PCA) was performed on the fractional abundances of the brGDGTs to analyze this. Principal component (PC1) described 57.4% of the variance in the dataset. BrGDGTs Ia, IIa, and IIa′ scored negatively on PC1, whereas all cyclic brGDGTs scored positively on PC1 (Fig. 3A). In line with this, the average number of cyclopentane moieties of the tetramethylated brGDGTs ($\#rings_{tetra}$ see Eq. (5)) significantly ($r^2 = 0.85$) positively correlated with PC1, with the exception of stations 16A, 26B, and 44A (Fig. 3C). BrGDGT IIIa and IIIa′ also scored positively on PC1. PC2 described an additional 19.0% of the variance in the dataset. The acyclic penta- and hexamethylated (both the 5- and 6-methyl) brGDGTs scored positively on PC2. Consequently, PC2 significantly ($r^2 = 0.95$) negatively correlated with the summed fractional abundance of tetramethyl brGDGTs (Fig. 3D) with the exception of the stations of transect A.

When the scores of the stations on PC1 and PC2 are considered (Fig. 3B), it is apparent that all stations in or close to the river mouth form one cluster (end-member A). The average brGDGT distribution of these sediments from the mouth of the river are dominated by Ia, and are

[1] Note that all GDGTs contain a macrocycle; here the term "acyclic" is used to indicate that these brGDGTs (i.e. Ia, IIa, IIa′, IIIa, and IIIa′) do not contain a cyclopentane moiety.

Table 3
Distributions of brGDGTs in surface sediments of stations in the Berau delta.

Station	Fractional abundance (% of total)										
	Ia	Ib	Ic	IIa	IIa′	IIb	IIb′	IIc	IIc′	IIIa	IIIa′
1C	63.4	10.4	3.0	7.6	8.6	1.4	2.0	0.3	0.3	1.2	1.7
2A	66.3	9.4	3.1	7.1	8.6	1.1	1.5	0.2	0.2	0.9	1.8
2B	67.7	9.6	3.1	6.6	8.0	1.0	1.4	0.2	0.2	0.9	1.4
3A	67.8	8.8	2.8	6.8	8.7	1.0	1.4	0.2	0.2	0.9	1.6
4B	54.9	12.6	7.8	6.0	7.5	1.0	1.2	0.6	0.4	3.3	4.6
8A	68.6	9.4	3.4	6.4	7.8	0.9	1.1	0.2	0.2	0.8	1.3
8B	68.2	8.8	2.8	6.8	7.9	1.1	1.5	0.2	0.2	1.0	1.5
10A	66.7	9.6	3.8	6.6	8.4	0.9	1.2	0.2	0.2	0.9	1.5
11A	67.0	9.2	3.3	6.8	8.6	0.9	1.3	0.1	0.2	0.9	1.5
11B	62.9	11.8	5.7	6.2	8.3	0.9	1.3	0.1	0.2	1.1	1.5
12A	64.6	10.9	4.8	6.2	8.7	0.9	1.1	0.1	0.2	1.0	1.5
12B	60.6	13.4	6.7	6.0	8.2	0.8	1.1	0.1	0.2	1.2	1.5
13B	63.3	11.5	4.8	6.7	8.6	0.9	1.2	0.1	0.2	1.3	1.5
14B	64.5	11.5	4.5	5.6	8.6	0.7	1.0	0.1	0.2	1.4	2.0
15B	66.7	10.1	3.5	6.2	8.7	0.9	1.2	0.1	0.2	0.9	1.5
16A	43.2	13.1	9.5	5.3	6.3	5.7	5.4	1.6	3.8	2.4	3.6
16C	69.3	8.3	2.4	7.5	8.1	0.9	1.1	0.2	0.2	0.9	1.2
18A	67.0	10.4	3.8	6.3	8.1	0.8	1.1	0.0	0.1	0.9	1.4
20A	57.9	14.0	8.6	6.3	7.1	0.8	1.3	0.2	0.4	1.5	1.9
21A	50.0	15.5	11.4	6.9	7.2	0.9	2.0	0.4	0.6	2.2	2.8
21B	48.9	15.7	11.9	7.0	7.0	1.0	2.1	0.5	0.6	2.3	3.0
22A	42.9	17.2	14.0	6.6	7.1	1.0	3.2	0.7	0.8	2.3	4.2
23B	41.6	17.7	14.9	5.9	6.6	1.2	3.7	0.8	0.9	2.3	4.4
23C	43.6	18.1	14.5	5.3	6.2	1.2	3.7	0.6	0.8	1.9	4.2
24A	29.2	23.4	21.5	4.2	4.5	4.5	3.6	2.1	0.9	2.5	3.5
25B	28.8	25.6	20.6	3.0	5.8	2.9	4.9	1.4	0.6	2.0	4.4
26B	56.8	9.4	5.2	5.8	7.2	3.9	2.7	1.3	1.3	2.5	3.9
27A	32.6	23.9	15.6	4.2	3.6	9.7	3.1	0.7	0.8	2.6	3.2
28A	35.5	23.7	17.1	4.5	4.8	3.9	3.1	0.9	0.7	2.3	3.4
29C	31.0	26.9	20.1	3.5	4.1	4.4	3.3	1.0	0.8	2.1	2.8
32A	56.2	16.5	3.6	8.4	7.8	1.1	1.5	0.2	0.4	2.1	2.0
33A	45.2	17.0	14.0	8.0	7.0	1.0	1.7	0.3	0.6	2.3	2.8
34A	42.1	18.1	15.2	7.8	7.0	1.1	2.2	0.4	0.7	2.4	3.1
35B	34.4	19.7	17.5	7.4	7.1	1.4	3.5	0.6	0.6	3.2	4.6
36B	32.1	19.1	16.5	7.6	8.4	1.4	4.2	0.8	0.8	3.6	5.6
37C	32.1	18.4	15.7	8.0	8.6	1.5	4.1	0.8	0.9	3.9	6.1
38A	33.8	18.4	15.2	7.2	8.1	1.4	4.6	0.7	0.9	3.5	6.1
39B	34.4	18.4	15.4	6.7	8.0	1.4	4.6	0.7	1.0	2.9	6.4
40A	35.2	18.5	15.0	6.3	8.3	1.3	4.3	0.6	0.9	2.8	6.8
41A	38.6	17.4	13.6	6.4	8.7	1.3	3.7	0.4	0.9	2.8	6.1
42A	37.9	13.5	9.8	6.1	8.5	1.5	3.1	0.4	0.6	5.9	12.6
43C	45.6	12.9	8.5	7.1	9.4	1.9	3.6	0.7	0.8	2.5	6.9
44A	40.6	12.5	8.9	7.2	8.6	4.3	4.0	1.8	1.2	3.4	7.5

characterized by a high value for the fractional abundance of all tetramethylated brGDGTs (%tetra; see Eq. (2)) and a relatively low value for $\#rings_{tetra}$ (Fig. 4B) in comparison to the average distribution for all Berau delta sediments (Fig. 4A). The scores for the stations on the transects (Fig. 3B) gradually move away from end-member A and are most dissimilar in the stations of transect A close to the shelf break (end-member B) with the exception of station 26B. Cyclic brGDGTs are far more dominant in the brGDGT distribution of the stations of end-member B (Fig. 4C). This is most apparent for the tetramethylated brGDGTs Ib and Ic but also the pentamethylated brGDGTs IIb, IIb′, IIc, and IIc′ show an increased fractional abundance. This marked change in distribution is also evident in the values for $\#rings_{tetra}$, which vary from 0.22 in the sediments in and close to the river mouth (end-member A) to 0.83 for the sediments close to the shelf break. The surface plot of $\#rings_{tetra}$ (Fig. 2F) shows that this change is gradual and that the highest values are generally found for sediments on the shelf with a water depth between 60 and 100 m. The deeper (>50 m) stations of transect B score positively on PC2 and, in that respect, behave differently from those of transect A.

3.3. GDGTs in deeper sediments

In the 1 m-long sediment core from station 11B the concentrations of brGDGT and crenarchaeol were 42.0 $\pm$ 6.1 ($n = 9$) and 211 $\pm$ 30 μg g TOC^{-1}, respectively (Table 2). BIT and TEX_{86} values were almost constant at

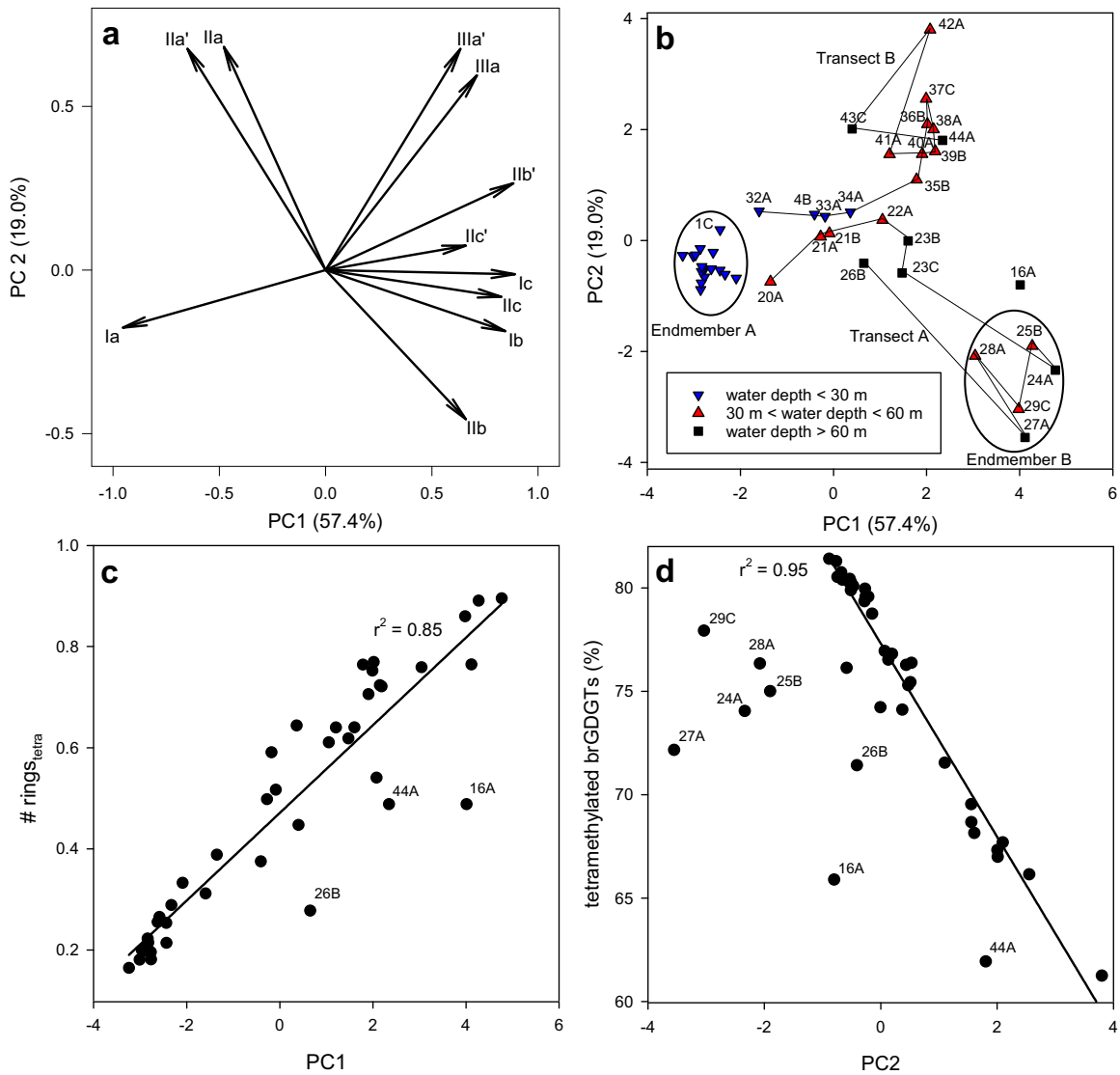

Fig. 3. PCA based on the fractional abundances of the 11 major brGDGTs in the sediments of the Berau delta. Panel A shows the scores of the 11 brGDGTs on the first 2 PCs. Roman numerals refer to the structure in the Appendix A. Panel B shows the scores for the stations. Different symbols indicate the water depth of the sites. The lines drawn are connecting the stations of Transects A and B (see Fig. 1). Based on the scores of the sites in this plot two end member distributions (A and B) have been defined which differ on the basis of the most negative and positive scores on PC1. Panel C shows a cross plot of PC 1 with $\#rings_{tetra}$. The linear correlation was calculated excluding stations 16A, 26B, and 44A. Panel D shows a cross plot of PC2 with the fractional abundance of the tetramethylated brGDGTs (Ia, Ib, and Ic). The linear correlation was calculated excluding the stations of transect A.

0.138 ± 0.004 and 0.588 ± 0.005, respectively (Table 2). The brGDGT distribution also did not show much variation; the fractional abundances of the tetramethylated branched and novel 6-methyl GDGTs were $80.9 \pm 0.4\%$ and $10.8 \pm 0.4\%$, respectively, while $\#rings_{tetra}$ was relatively constant at 0.293 ± 0.009 (Table 2).

4. DISCUSSION

4.1. The delivery of terrestrial organic matter over the Berau shelf

Tropical rivers are typically transporting a lot of eroded soil OM and higher plant remains and, consequently, suspended particulate matter (SPM) in tropical rivers is therefore depleted in ^{13}C. For example, $\delta^{13}C_{TOC}$ values of SPM in the Amazon are −29.3‰ (Kim et al., 2012) and in the Kapuas river in West Kalimantan ca. −29.5‰ (Loh et al., 2012). The Berau River also contains a high load of suspended matter (Buschman et al., 2012) and, although we did not study SPM from the river, the $\delta^{13}C_{TOC}$ value (−30.0‰) of the surface sediment of the most upstream station (1C; Fig. 1) suggests that it is predominantly comprised of terrestrial OM (Tyson, 1995). It remains ambiguous whether this OM is only derived from eroded soil OM and higher plant remains or that OM produced in the river itself also contributes since the $\delta^{13}C_{TOC}$ of riverine aquatic OM usually does not substantially differ from OM in soil or

higher plants (e.g. Cloern et al., 2002). This is entirely different for OM produced in marine environments, which is substantially enriched in ^{13}C ($\delta^{13}C_{TOC}$ = ca. −20‰; Tyson, 1995). The large gradient in $\delta^{13}C_{TOC}$ indicates that particulate terrestrial organic matter is only transported over relatively short distances in the Berau River delta. The isosurface plot of $\delta^{13}C_{TOC}$ (Fig. 2B) reveals that in sediments from a water depth >25 m values of $\delta^{13}C_{TOC}$ have increased to >−24‰ and that at the shelf break they approach the marine OM end-member. Consequently, only a minor part of the terrestrial particulate OM is transported over distances >25 km from the river mouth, in good agreement with the reported extension of the Berau River plume (Renema, 2006). Analysis of a short core at station 11B revealed that $\delta^{13}C_{TOC}$ remained quite constant over the last 100 yr or so (Table 2). Since both the sedimentation rate (1–3 cm yr^{-1}) and the TOC content (Fig. 2A) are high in this area still a substantial amount of terrestrial OM is buried on this part of the shelf.

This behavior of terrestrial OM in the Berau delta is confirmed by the GDGTs; the highest concentrations of acyclic brGDGTs, which have often been used as tracers for terrestrial OM (Hopmans et al., 2004; Schouten et al., 2013b), are found in the sediments in or closest to the river mouth (Fig. 2D). Sediments of stations further away from the river show a lower concentration of acyclic brGDGTs but a substantial increase in the concentration of crenarchaeol (Fig. 2C), derived from marine Thaumarchaeota. This results in a sharp gradient in the values of the BIT index over the shelf (Fig. 2E), following a pattern similar

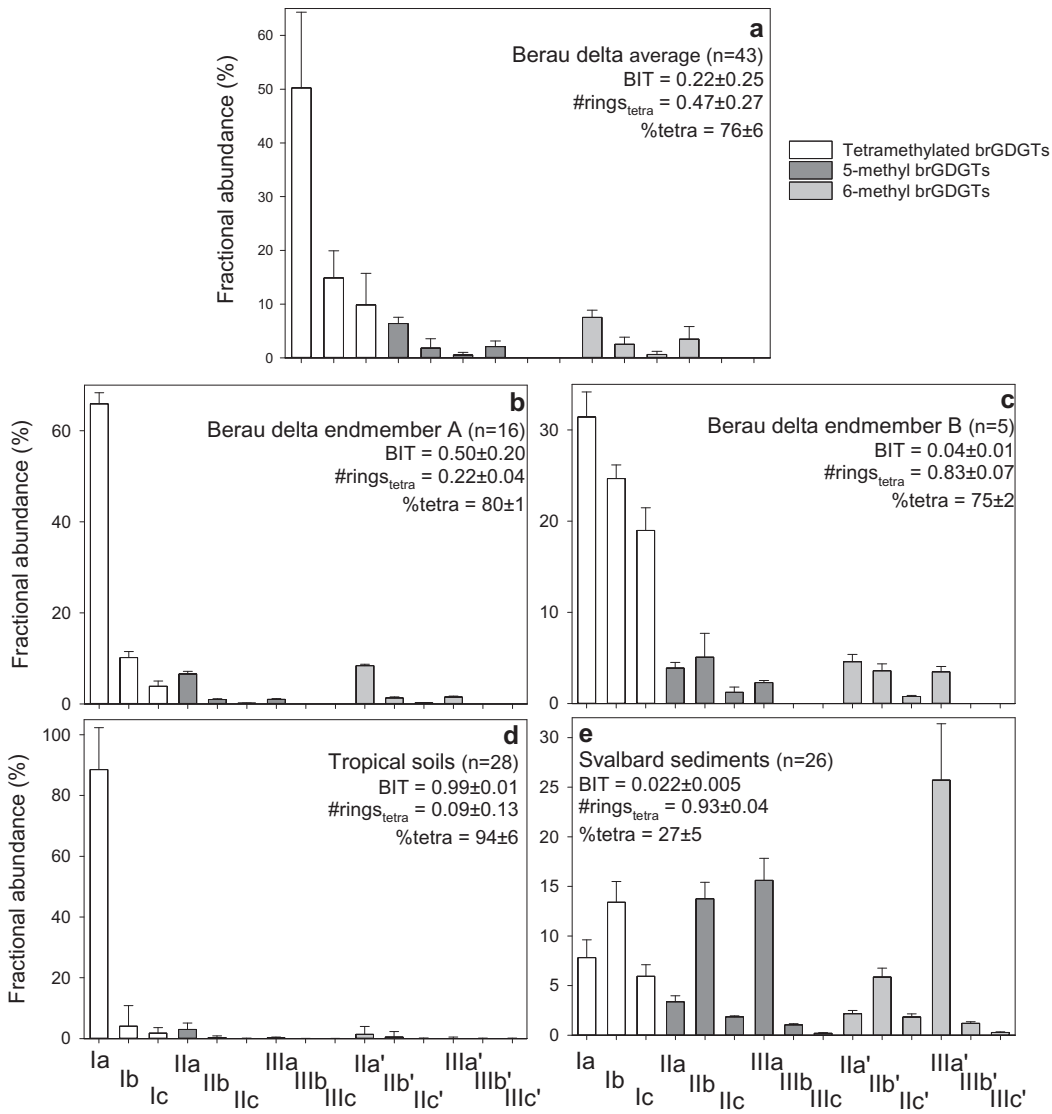

Fig. 4. Bar plots showing the fractional abundance (expressed as the percentage of the total) of the 15 brGDGTs (see Appendix A for structures) in (A) the sediments of the Berau delta, (B) end-member A of the Berau delta sediments, (C) end-member B of the Berau delta sediments, (D) tropical soils (data from De Jonge et al., 2014a), and (E) Svalbard sediments (data from Peterse et al., 2009a; reanalyzed using the new UHPLC method, see experimental methods). All distributions represent the average of a number of samples (as indicated). The error bar reflects ± 1 SD. The color of the bars refers to the structure of the brGDGTs (see legend). For all sample sets the average of the BIT index, #rings$_{tetra}$ and %tetra is indicated with the SD.

to that of $\delta^{13}C_{TOC}$ (Fig. 2B). A spational distribution similar to that of the acyclic brGDGTs has been noted for the aromatic hydrocarbon perylene (Booij et al., 2012) with the highest concentration in sediments of the most upstream station and rapidly declining concentrations in sediments of the river mouth at greater water depth. This was interpreted as indicating a terrestrial origin for perylene in this setting. When $\delta^{13}C_{TOC}$ is cross-plotted with the BIT index a logarithmic correlation ($R^2 = 0.91$) is observed (Fig. 5A). A similar behavior of BIT has been reported for the Arctic shelf (Sparkes et al., 2015) and also other shelf settings show a relationship between BIT and $\delta^{13}C_{TOC}$ (Fig. 5A).

4.2. Provenance of brGDGTs

The rapid decline of the concentration of the brGDGTs goes together with a marked change in their distribution (Figs. 4B, C, and 3C). In the most upstream stations the distribution of the brGDGTs is dominated (i.e. ca. 65% of total brGDGTs) by brGDGT Ia (Fig. 4B). This is a distribution that is characteristic for tropical soils (e.g. Weijers et al., 2006; Sinninghe Damsté et al., 2008), although in tropical soils the dominance of Ia is even more extreme (i.e. 83% of total brGDGTs on average; Fig. 4D). Since tropical soils are often acidic, cyclic brGDGTs, that are predominantly formed at pH > 7, are minor, and the high temperature leads to a low degree of methylation, overall resulting in the dominance of the acyclic tetramethyl brGDGT Ia (cf. Weijers et al., 2007b). Unfortunately, no soils from the watershed of the Berau River were available to determine their brGDGTs distribution. It has been well documented that even in tropical rivers that carry a high load of SPM, primarily from soil erosion, the distribution of brGDGT in the SPM may differ from that of the soils in the watershed due to in-situ production of brGDGTs in the river. In the Amazon river it was shown that the contribution of riverine in-situ production varied depending on the season (Zell et al., 2013a,b); at times of high rainfall and increased soil erosion the SPM brGDGT distribution was similar to that of the soil from the watershed, whereas in dry seasons the brGDGTs in the SPM represented a mixture of soil-derived and in-situ produced brGDGTs. There are no comparable studies of Indonesian rivers but Tierney and Russell (2009) compared the brGDGT distribution of sediments of a number of small rivers entering Lake Towuti on the island of Sulawesi (Indonesia; Fig. 1) with those of the tropical soils in the watershed of the lake. This is an area that is nearby Kalimantan and experiences the same climatic regime. Tierney and Russell (2009) noted a substantially different distribution of brGDGTs in the river sediments compared to the soils (Fig. 6A and B) and attributed this to riverine in situ production of brGDGTs. Comparison of these distributions with that of end-member A in the Berau Delta (Fig. 6C) indeed suggests that the brGDGTs in the sediments of the stations in and close to the river mouth reflect a mixture of soil-derived and riverine in-situ produced brGDGTs.

In the sediments of the stations further away from the mouth of the river, closer to the shelf break, concentrations of brGDGTs are lower and their distribution differs markedly from that of end-member A. Their distribution is still dominated by tetramethylated brGDGTs but, in addition to the acyclic brGDGT Ia, the cyclic brGDGTs Ib and Ic are also abundant (Fig. 4c). Also, for the 5- (IIb and IIc) and 6-methyl (IIb′ and IIc′) pentamethylated brGDGTs an increased relative abundance of cyclic brGDGTs is observed but not so for the hexamethylated brGDGTs (IIIb, IIIc, IIIb′, and IIIc′). This is similar to what has been observed for surface sediments in a Svalbard fjord (Fig. 4e) with respect to the high fractional abundance of cyclic brGDGTs. Peterse et al. (2009a) compared the distribution of Svalbard fjord sediments with those of soils and attributed the unusual dominance of cyclic brGDGTs to in-situ production in the marine sediments, which was supported by the higher TOC-normalized concentrations of brGDGTs in sediments compared to the soils. Since the pH of marine sediment pore waters is typically around 8, in-situ production of brGDGTs would generate a brGDGT distribution dominated by cyclic brGDGTs since pH is the major environmental control on the degree of cyclization of

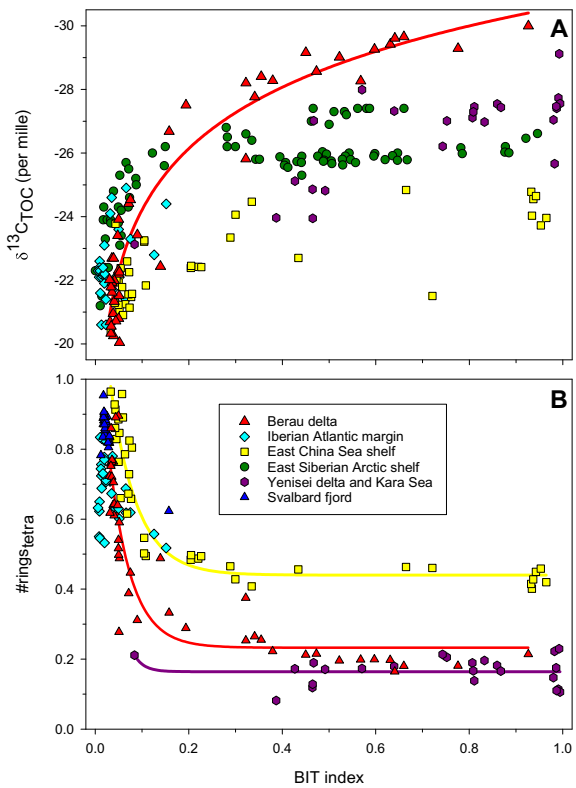

Fig. 5. Cross plots of (A) BIT index $\delta^{13}C_{TOC}$ (‰) for the Berau shelf, showing a logarithmic relation (thick red line; $R^2 = 0.91$), and (B) BIT index versus $\#rings_{tetra}$. For reference, surface sedimentary datasets from other river influenced shelf settings are shown, i.e. East China Sea shelf system (data from Zhu et al., 2011), the Iberian Atlantic shelf (data from Zell et al., 2015), the East Siberian Arctic shelf (data from Sparkes et al., 2015), and the Yenisei delta and Kara Sea (data from De Jonge et al., 2015). Panel B also shows the data for Svalbard fjord sediments (Peterse et al., 2009a; reanalyzed using the new UHPLC method, see experimental methods). (For interpretation of the references to color in this figure legend, the reader is referred to the web version of this article.)

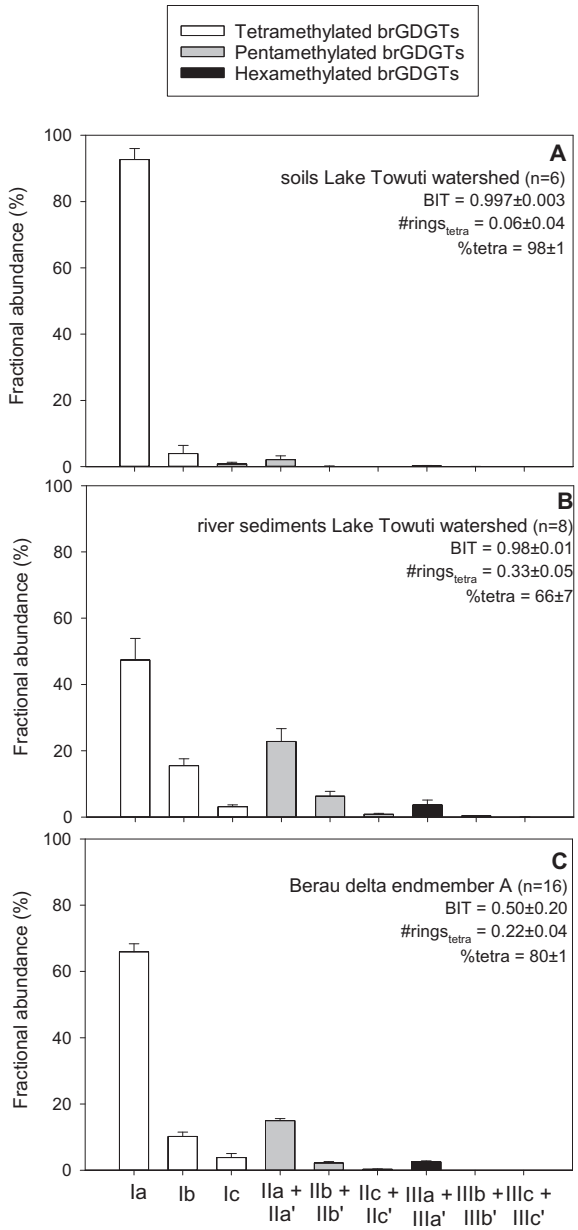

Fig. 6. Bar plots showing the fractional abundance (expressed as the percentage of the total) of brGDGTs in (A) soils of the watershed of Lake Towuti (data from Tierney and Russell, 2009), (B) sediments of small rivers entering Lake Towuti (data from Tierney and Russell, 2009), and (C) end-member A of the Berau delta sediments (this study). All distributions represent the average of a number of samples (as indicated). The error bar reflects ± 1 SD. Italic numbers refer to structures in the Appendix A. For all sample sets the average of the BIT index, #rings$_{tetra}$ and %tetra is indicated with the SD. Note that the data obtained by Tierney and Russell (2009) was obtained by an analytical method that did not separate the 5- and 6-methyl brGDGTs and the presented data thus reflect the sum of these isomers. For reasons of comparison, the data of the Berau delta are also presented in this way.

brGDGTs (Weijers et al., 2007b; Peterse et al., 2010). The same observation has been used by Weijers et al. (2014) to conclude that brGDGTs in distal marine sediments are also predominantly derived from in-situ production. Schoon et al. (2013) also noted that the degree of cyclization of in-situ produced brGDGTs in lakes strongly depends on the pH of the lake water, although the cyclic brGDGTs were never as dominant as in the sediments from the Svalbard fjord. Re-analysis of the Svalbard fjord sediments with the UHPLC method able to separate the 5- and 6-methyl brGDGTs (Fig. 4e) allowed a detailed comparison with that of end-member B of the Berau delta (Fig. 4c). This shows that the 5- and 6-methyl brGDGTs behave similarly; the relatively high fractional abundance of the cyclic brGDGTs is observed for penta- but not for the hexamethylated brGDGTs, just as observed for the end-member B of the Berau delta.

Overall this indicates that the sediments that are more distant from the river contain predominantly marine, sedimentary in-situ produced brGDGTs produced at a higher pH, resulting in a distribution in which cyclic brGDGTs are abundant. The shallow waters of the Berau shelf are warm (ca. 30 °C) and this probably explains why their distribution are still dominated by tetramethylated brGDGTs, which are preferentially formed at high temperatures (cf. Weijers et al., 2007b; Tierney et al., 2010). This indirectly supports the case for in-situ production.

On the shelf a gradual transition from end-member A to B is seen. This is clearly seen for transects A and B where the score on PC1 and #rings$_{tetra}$ increase with increasing distance from the coast although maximum values for #rings$_{tetra}$ are not reached at the end of both transects but in a specific band (Fig. 2F), where apparently conditions for in-situ production of brGDGTs are optimal. A clear distinction between transects A and B lies in the substantially declined fractional abundances of tetramethylated brGDGTs along transect B, resulting in positive scores on PC2 (Fig. 3). The reason for this difference remains unclear.

4.3. Other shelf settings

To examine if the spatial heterogeneity observed for the brGDGTs at the Berau shelf is more generally observed for river-deltaic systems, data available in the literature were examined. Various other river-influenced shelf settings have been studied with respect to the spatial distribution of brGDGTs (e.g. Kim et al., 2006, 2010b; Walsh et al., 2008; Schmidt et al., 2010; Zhu et al., 2011; Wu et al., 2014; Zell et al., 2014a,b, 2015; De Jonge et al., 2015; French et al., 2015; Lü et al., 2015; Selver et al., 2015; Sparkes et al., 2015). However, in most cases only the relative abundance of the most abundant acyclic brGDGTs (Ia, IIa and IIa', IIIa and IIIa') but not of the cyclic brGDGTs was reported. In other cases the spatial grid of sampling is relatively poor. This makes comparison with the data reported here for the Berau delta impossible. Comparisons are also complicated because almost all data on such systems have been acquired with methods that did not separate the 5- and 6-methyl brGDGT isomers as applied here. Therefore, the comparison is limited to three other river-influenced shelf systems, i.e. the East China Sea shelf, the Iberian Atlantic Ocean shelf, and the Yenisei delta and Kara Sea.

Zhu et al. (2011) reported the distributions of brGDGTs in surface sediments from the Lower Yangtze River and

East China Sea shelf at approximately 30°N. Concentrations of brGDGTs declined rapidly with increasing distance from the mouth of the Yangtze River, resulting in declining values of the BIT index from >0.8 in river sediments to values <0.20 in shelf sediments at a water depth > ca. 50 m (Fig. 7). At the same time, Zhu et al. (2011) also noted a marked change in the distribution of the brGDGTs (their Fig. 7). In the open shelf setting, cyclic brGDGTs were relatively abundant compared to sediments from the river and estuary. This is clearly visible in the isosurface plot of #rings$_{tetra}$ (Fig. 7C); values increase with increasing distance from the coast and approach the maximum values observed in Svalbard fjord sediments (ca. 1.0; Fig. 8B). The increase in #rings$_{tetra}$ from values <0.5 in the river and shallow sea sediments starts at ca. 50 m water depth and reaches maximum values at ca. 100 m (Fig. 8B). This situation is comparable to that observed for the Berau shelf. (Figs. 2B and 8B). The changes in the BIT index and the distribution of brGDGTs go in parallel (Fig. 5B) and are indicative of two distinct sources of brGDGTs: a soil/riverine source and marine in-situ production. Even the shelf water depth at which these changes occur are comparable for both systems (Fig. 8B). This makes sense since the river supply of suspended matter is an important control for both water depth on the shelf (i.e. sediment supply) and for the delivery of brGDGTs.

Zell et al. (2015) reported the distributions of brGDGTs in surface sediments from five transects on the Iberian Atlantic shelf and slope at approximately 40°N (Fig. 9A), which is influenced by the Douro and Tagus rivers, and some smaller rivers. At this shelf setting concentrations (normalized on TOC) of brGDGTs declined rapidly with increasing distance from the coast, whereas crenarchaeol concentrations are generally higher in the open marine environment (Zell et al., 2015). This results in rapidly declining values of the BIT index varying from 0.6 to 0.9 in SPM of the Tagus river (Zell et al., 2014a) to values of ca. 0.10–0.15 in shallow sediments close to the mouth of the Douro and Tagus (Fig. 9B). In the sediment from the shelf and slope values of the BIT index further decrease with increasing water depth (Figs. 8A and 9B). Also at the Iberian Atlantic shelf an increase in #rings$_{tetra}$ is noted with increasing water depth (Figs. 8B and 9C), as is observed for the shelves of the Berau River (Fig. 2F) and the East China Sea (Fig. 7C), reaching values of ca. 0.8. This dataset also indicates that, at least for this system, #rings$_{tetra}$ in sediments in deeper water gradually decreases again (Fig. 8B). This may indicate that an increasing fraction of the brGDGTs in sediment from deeper waters are sourced by continental brGDGTs, which have been transported over long distances, potentially by strong adsorption to terrestrial particles delivered by rivers (e.g. De Jonge et al., 2014) or by wind (e.g. Fietz et al., 2013). The strong adsorption may protect brGDGTs from degradation as suggested for surface sediments from the Kara Sea shelf (De Jonge et al., 2014). This would also imply that marine in-situ production of brGDGTs is relatively abundant in shallow, but not too shallow, shelf sediments (Fig. 8B). This would be in line with the general idea that the bacteria that produce brGDGTs (and related lipids) are heterotrophs (Pancost and Sinninghe Damsté, 2003; Oppermann et al., 2010; Weijers et al., 2010; Sinninghe Damsté et al., 2011, 2014). Marine primary productivity and consequently the organic matter flux to the sediments is generally higher at the shelf than in slope and abyssal plain settings and this may "fuel" benthic in-situ production of brGDGTs. Marine in-situ production may also take place in the water column but the few studies that have reported brGDGT distributions in marine SPM in oxic waters (Zell et al., 2014a,b; De Jonge et al., 2015) do not report the high degree of cyclization that is characteristic for shelf sediments (e.g. Figs. 4C, E and 8B).

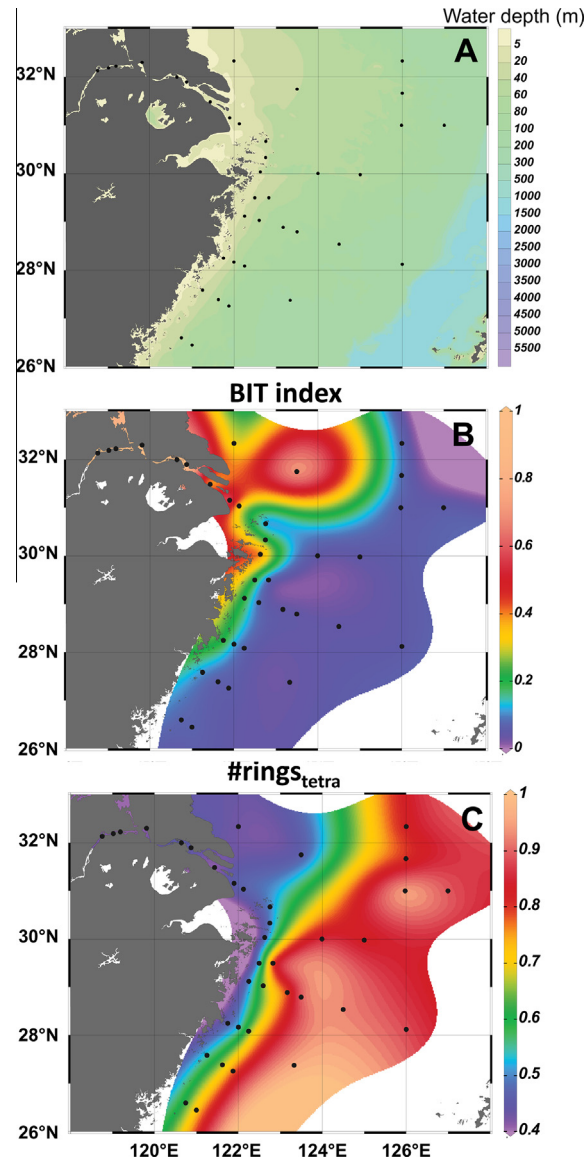

Fig. 7. Isosurface plots for (A) water depth (m) for the East China Sea shelf system, where the Yangtze river discharges a large amount of suspended matter, and (B) BIT index, and (C) #rings$_{tetra}$ in the surface sediments. Data are from Zhu et al. (2011). Note the large increase in #rings$_{tetra}$ for sediments at a water depth of >50 m.

One other river-influenced shelf setting that has recently been studied with respect to the distribution of brGDGTs using the new analytical methodology is the Yenisei delta

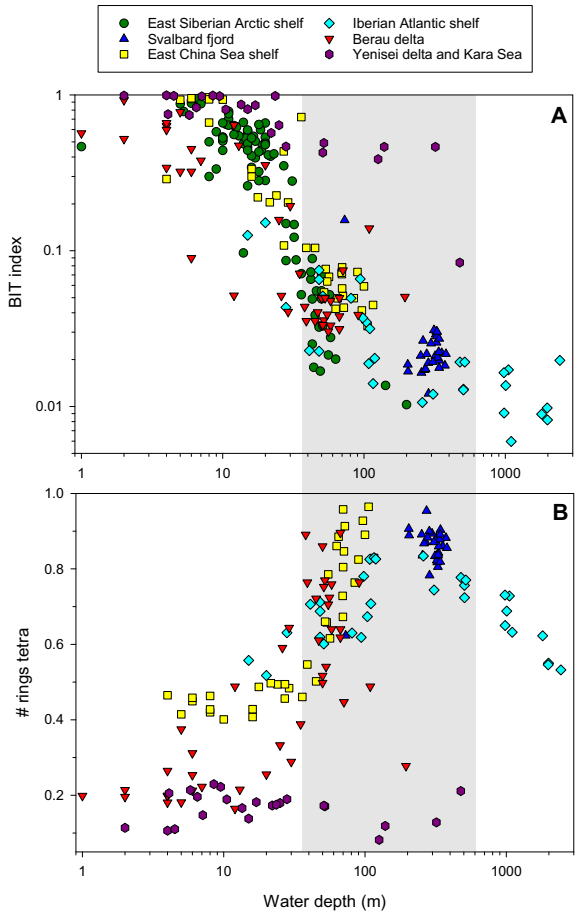

Fig. 8. Cross plots of BIT index (A) and #rings$_{tetra}$ (B) vs. water depth (in m) for surface sediments of the Berau delta, Svalbard fjord sediments (data from Peterse et al., 2009a; reanalyzed using the new UHPLC method, see experimental methods), Iberian Atlantic Shelf sediments (data from Zell et al., 2015), East China Sea Shelf sediments (data from Zhu et al., 2011), and the Yenisei delta and Kara Sea (data from De Jonge et al., 2015). The gray area indicates the water depths at which, at least for these datasets (except for the Kara Sea), elevated values for #rings$_{tetra}$ are noted, interpreted to be caused by in-situ production in marine sediments. Note the logarithmic scale for the X-axis (water depth) and the Y-axis (BIT index) for (A). Values for the BIT index measured in different laboratories cannot be compared directly (Schouten et al., 2013a), indicating that in this plot only the trends for the BIT index in the sediments from the East China Sea shelf and the East Siberian Arctic shelf can be compared with the data sets produced at the NIOZ laboratory.

and Kara Sea (De Jonge et al., 2015). This shelf sea in the Arctic region is influenced by organic matter delivery from the Yenisei and Ob river. Surface sediments in the Kara Sea did not reveal the high degree of cyclization as observed in other shelf seas (Fig. 8B). This may have two reasons. Firstly, only a limited number of samples were studied, mostly derived from shallow waters (water depth < 30 m) where the increase in #rings$_{tetra}$ is not seen yet (Fig. 8B). Secondly, in this shelf system the amount of brGDGTs delivered by the large rivers may overwhelm in-situ production in the marine sediments. It is noteworthy that in this system the values for the BIT index are still high and those of #rings$_{tetra}$ are still low at greater water depth (Fig. 8). It has been proposed that erosion of coastal cliffs may be an additional source for brGDGTs in the Kara Sea (De Jonge et al., 2015), which also may be part for the deviating behavior of the Kara Sea. It is noteworthy, however, that in older, Holocene sediments from the St Anna through in the Kara Sea (at a present day water depth of 473 m) #rings$_{tetra}$ approaches 0.75 (De Jonge et al., 2016). This suggests that during the post-glacial sea level rise, the water depth at a certain interval was optimal for generating a clear marine in-situ brGDGT "signature".

4.4. How to discern sources of brGDGTs in shelf sediments?

For the application of brGDGTs in coastal marine sediments as proxies in palaeoenvironmental studies, it is essential to have knowledge about the sources of the brGDGTs. Improved estimates of mean annual air temperature (MAT) and soil pH can be made using the new soil calibrations (De Jonge et al., 2014a). However, these can only be applied in coastal sediments when the brGDGT are predominantly derived from soil erosion. The estimate for MAT based on the MBT′5Me index (De Jonge et al., 2014a) in the area of the Berau delta that receives a substantial terrestrial organic matter input (i.e. end-member A) is ca. 20 °C. This is substantially lower than the present-day MAT in East Kalimantan of ca. 26–27 °C (Hansen et al., 2010), which is most probably due to the admixture of riverine produced brGDGTs (see Section 4.2). In lakes it has also been noted that application of soil calibrations for brGDGT temperature proxies often leads to estimated temperatures that are too low (e.g. Tierney et al., 2010; Zink et al., 2010; Loomis et al., 2011). This is probably because the brGDGT-producing bacteria in aquatic environments have a response to environmental parameters (temperature, pH) that is different from those in soil. Consequently, lake calibrations for brGDGTs have been proposed (e.g. Pearson et al., 2011; Sun et al., 2011; Loomis et al., 2012) but they remain somewhat problematic since lakes often receive contributions from two main sources, i.e. soil erosion (e.g. Niemann et al., 2012; Loomis et al., 2014) and in-situ production in the lake itself (e.g. Buckles et al., 2014; Weber et al., 2015) in varying ratios. It is, therefore, important to be able to decide if brGDGTs in aquatic environments are derived predominantly from soil erosion or not. Initially, it was thought that the BIT index could be used to this end (Hopmans et al., 2004). However, now that we know that brGDGTs are also produced in-situ in rivers (e.g. Tierney and Russell, 2009; Zell et al., 2013a,b, 2014a, b), in lakes (e.g. Sinninghe Damsté et al., 2009; Buckles et al., 2014; Weber et al., 2015), in the marine water column (e.g. Liu et al., 2014; Xie et al., 2014; Zell et al., 2014a,b; De Jonge et al., 2015), and in marine sediments (e.g. Peterse et al., 2009a; Zhu et al., 2011), the BIT index is no longer of use in this respect. Is it possible to make this distinction on the basis of the composition of the brGDGTs itself?

Using the improved chromatography to separate the 5- and 6-methyl brGDGTs (De Jonge et al., 2013; Hopmans et al., 2016), the compositions of brGDGTs in

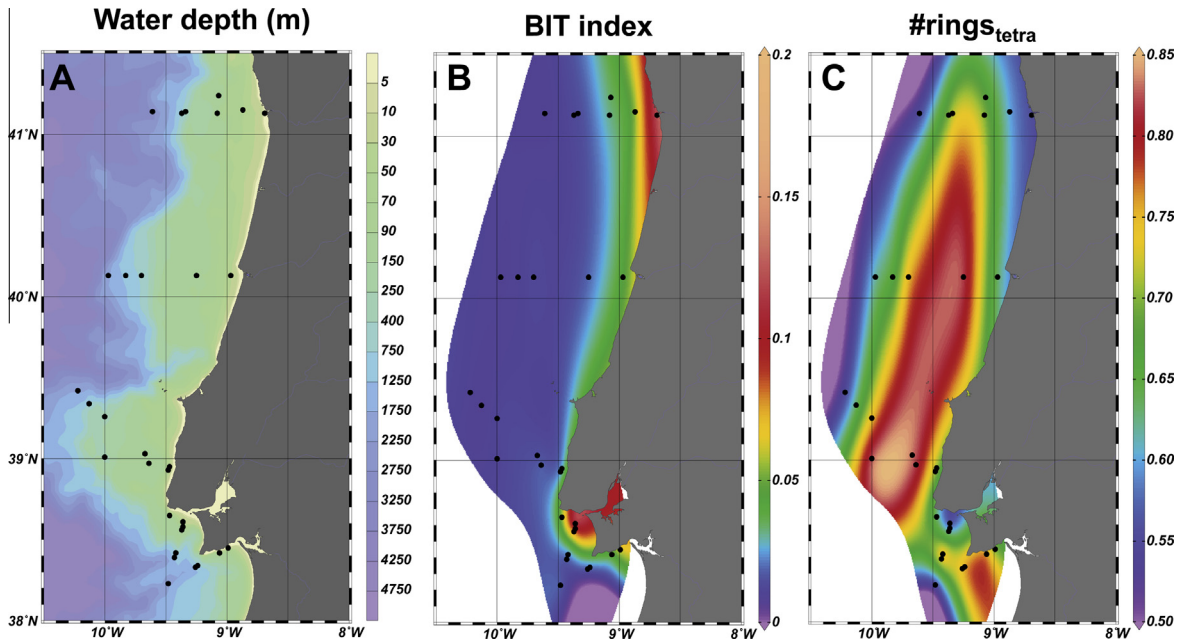

Fig. 9. Isosurface plots for (A) water depth (m) for the Iberian Atlantic Ocean shelf system, where the Douro and Tagus and some smaller rivers discharge suspended matter on the shelf, and (B) BIT index, and (C) #rings$_{tetra}$ in the surface sediments. Data are from Zell et al. (2015). Note the gradual increase in #rings$_{tetra}$ for sediments at a water depth of 20–200 m and the subsequent decrease at greater water depth.

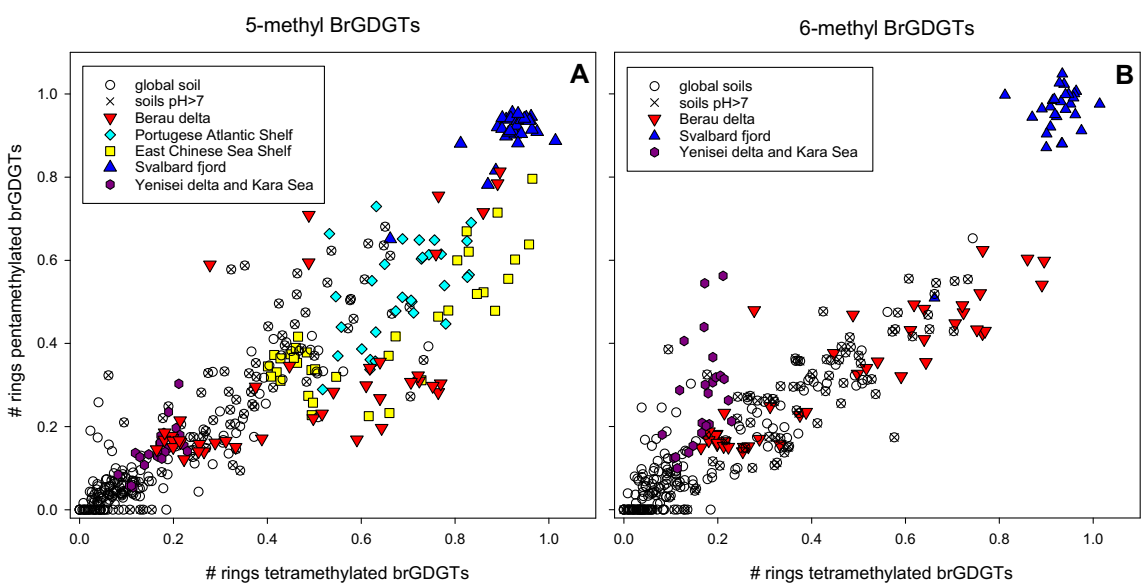

Fig. 10. Cross plots of the average number of cyclopentane moieties for tetramethylated brGDGTs (#rings$_{tetra}$) versus those for (A) 5-methyl and (B) 6-methyl brGDGTs. Data sets used are global soils (De Jonge et al., 2014a), Berau shelf sediments (this study), Svalbard fjord sediments (Peterse et al., 2009a; reanalyzed using the new UHPLC method, see experimental methods), the Yenisei delta and Kara Sea (data from De Jonge et al., 2015), Iberian Atlantic Shelf sediments (Zell et al., 2015), and East China Sea Shelf sediments (Zhu et al., 2011). Note that in the latter two datasets the 5- and 6-methyl brGDGTs were not individually quantified. The values plotted in (A) actually, therefore, represent #ring$_{penta}$ for the sum of the 5- and 6-methyl brGDGTs for these datasets. Soils with a pH > 7 are indicated by a separate symbol.

river-influenced shelf environments can be compared with those in soils (De Jonge et al., 2014a) in various ways. Firstly, we can compare the values for #rings of the tetramethylated and 5- and 6-methyl pentamethylated brGDGTs. In the global soil dataset, these values generally do not exceed 0.4 for soils with a measured pH of <7 (Fig. 10), whereas soils with a pH > 7 may reach values up to 0.7. In five sets of coastal sediments a wide variety of values is observed. In the sediments of the Svalbard fjord these values are generally high (0.8–1.0; Fig. 10), clearly above those of the soil data set. In the sediments of the Yenisei delta and Kara Sea, they remain <0.3, except for #ring$_{penta}$ of the 6-methyl brGDGTs, which occasionally reaches almost 0.6 (Fig. 10). For the Berau shelf sediment a wide variety of values (0.2–0.9) is observed. The same is evident for the sediments of South China Sea shelf and the Iberian

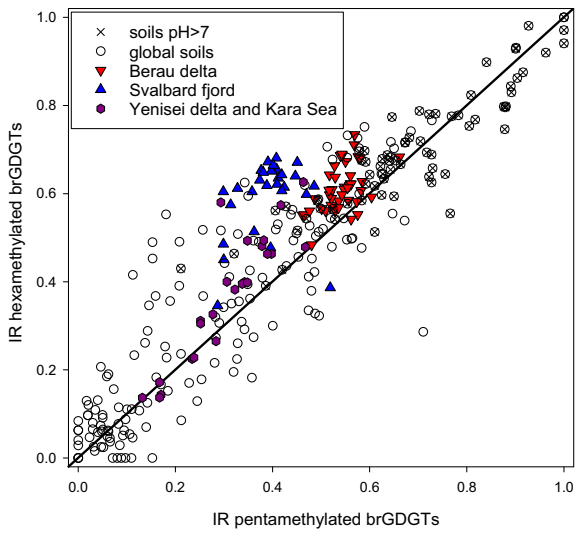

Fig. 11. Cross plots of the isomer ratio (IR) for the penta- and hexamethylated brGDGTs. Data sets used are global soils (De Jonge et al., 2014a), Svalbard fjord sediments (Peterse et al., 2009a; reanalyzed using the new HPLC method), the Yenisei delta and Kara Sea (data from De Jonge et al., 2015), and Berau shelf sediments (this study).

Atlantic Ocean shelf with values in the same region. Overall, all datasets generally reveal a clear, almost 1:1, relationship between $\#rings_{tetra}$ and $\#rings_{penta}$. From these plots it is evident that brGDGTs, where the average number of rings exceeds 0.7, cannot fully derive from soil erosion.

A second approach is to look at the IRs (see Eqs. (8) and (9)) as previously defined by De Jonge et al. (2014b). Soils cover the full range of values (0–1) for IR for both the penta- and hexamethylated brGDGTs (Fig. 11) as previously described by De Jonge et al. (2014a). High pH soils tend to have high values for IR (Fig. 11). In the Svalbard, the Berau delta, and the Yenisei delta and Kara Sea sediment sets much less variation in values for IR is observed. This is remarkable since all of the sediments from the Svalbard fjord and some of the Berau delta have values for $\#rings_{tetra}$ and $\#rings_{penta}$ that exceed those in any of the soils (Fig. 9). Both the degree of cyclisation of brGDGTs (Weijers et al., 2007b; Peterse et al., 2010, 2012; De Jonge et al., 2014a) and the dominance of 6-methyl brGDGTs (De Jonge et al., 2014a) is thought to be an adaptation of the membranes of brGDGT-producing bacteria to increasing pH. Apparently, there is a difference in response between soil and aquatic environments; in soils the IR reaches 1 at high pH, whereas $\#rings_{tetra}$ and $\#rings_{penta}$ remain <0.7. In coastal sediments with alkaliphilic pore waters the IR stays <0.7 (Fig. 11), while $\#rings_{tetra}$ and $\#rings_{penta}$ may reach values as high as 1 (Fig. 10). In river waters, however, IR may be much higher; De Jonge et al. (2014b) reported values for IR up to 0.9 for brGDGTs in SPM in the Yenisei river, interpreted as evidence for in-situ production in the more alkaline waters of the Yenisei river. In any case, IR is not helpful in identifying brGDGTs in coastal sediments that are not derived from soil since soils cover the full range of IR values (0–1; Fig. 11).

A third possibility would be to look at the degree of methyl branching of the brGDGTs. When the fractional abundances of the summed tetra-, penta-, andhexamethylated brGDGTs in soils are plotted in a ternary diagram (Fig. 12A), it is evident that the soil brGDGT composition generally lies within clearly defined boundaries. This becomes even more evident when the fractional abundances of the tetramethylated brGDGTs are plotted against those of the penta- (Fig. 12B) and hexamethylated (Fig. 12C)

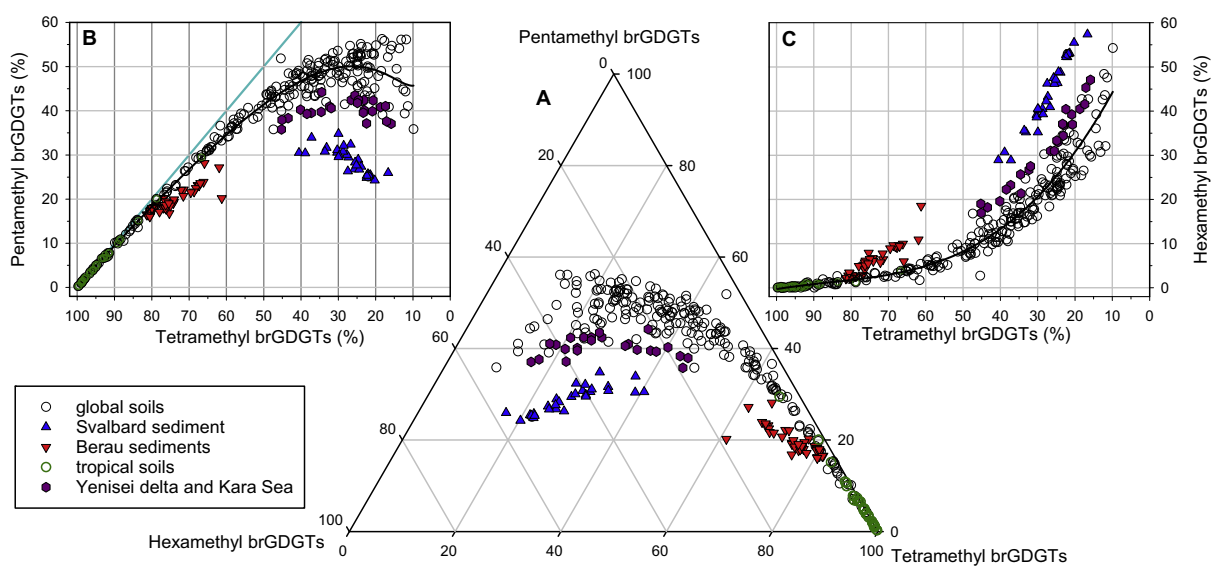

Fig. 12. General composition of brGDGTs in soils and shelf sediments. (A) Ternary diagram showing the fractional abundances of tetra- (Ia-c), penta- (IIa-c plus II′a-c), and hexamethylated (IIIa-c plus III′a-c) brGDGTs. (B) and (C) Cross plots of the fractional abundance of the tetramethylated brGDGTs versus the penta- and hexamethylated brGDGTs, respectively. Note the inverted scale on the X-axis for these plots. The straight line in (B) describes mixtures only composed of tetra- and pentamethylated brGDGTs. Data sets used are global soils (De Jonge et al., 2014a), Svalbard fjord sediments (Peterse et al., 2009a; reanalyzed using the new UHPLC method), the Yenisei delta and Kara Sea (data from De Jonge et al., 2015), and Berau shelf sediments (this study).

brGDGTs. Temperature is known to have a marked effect on the degree of methyl branching of brGDGTs in soils (Weijers et al., 2007b; Peterse et al., 2009b; De Jonge et al. 2014a). This is why tropical soils are dominated by tetramethylated brGDGTs (Figs. 4D and 12). Taking this as a starting point, it is clear from Fig. 12B that a decreasing fractional abundance of the tetramethylated brGDGTs, most likely caused by a lower MAT, is initially compensated by an increase of the fractional abundance of the pentamethylated brGDGTs (i.e. the fitted line is quite similar to the line that describes mixtures only composed of tetra- and pentamethylated brGDGTs; Fig. 12B). Only when fractional abundances of the tetramethylated brGDGTs become <50%, hexamethylated brGDGTs become relatively important (i.e. over 10%). From there on, there is somewhat more variation but the brGDGT composition in soils remains within clear limits (Fig. 12). When the data for the Svalbard fjord are plotted in these diagrams, it becomes immediately clear that the brGDGT produced in-situ in these marine sediments have a composition that is rather different from that of soils (Fig. 12). The sediments of the Berau delta are plotting more closely to the soil data but most Berau delta sediments are clearly deviating from the distinct trend between %tetra and %penta observed for the soil data set (Fig. 12B). The sediments from the Yenisei delta and Kara Sea are plotting most closest to the soil data. In fact, some soils have a similar brGDGTs composition. As discussed other parameters (BIT index, $\#rings_{tetra}$, $\#rings_{penta}$) are consistent with a predominant terrestrial origin for brGDGTs in this setting. The application of these "degree of methyl branching" plots seems to hold some promise in assessing a predominant soil origin for brGDGTs in coastal marine sediments and, perhaps, lakes. This may assist in the application of brGDGTs in palaeoenvironmental studies. It should, however, be emphasized that this can only be performed with datasets that have been acquired by a proper separation of the 5- and 6-methyl brGDGTs. Although, at first sight, this may seem odd since only %tetra, %penta, and %hexa (where 5- and 6-methyl isomers are summed; see Eqs. (2)–(4)) are used, the improved separation of especially the hexamethylated brGDGTs results generally in an increased %hexa, resulting in substantially improved separation of the various datasets. Application to more datasets will need to be performed to determine if this may be of additional help in the assessment of the origin of brGDGTs in coastal marine sediments.

5. CONCLUSIONS

(1) This high-resolution study of the Berau delta shows that, despite the extensive transport of eroded soil material by the river to the sea, the brGDGTs are only deposited on a relatively small part of the shelf.
(2) The brGDGT distribution in sediments deposited in and close to the mouth of the Berau River indicate that they represent a mixture of soil-derived and river in-situ produced brGDGTs.
(3) On the shelf, in the area not under the direct influence of the Berau River, in-situ produced brGDGTs become dominant. These are characterized by a much higher abundance of cyclic brGDGTs, resulting in high values for $\#rings_{tetra}$. Tetramethylated brGDGTs still dominate, most probably because the Berau shelf waters are warm. Benthic brGDGT producing microbial communities, therefore, still seem to follow a similar adaptation to temperature as those in soil.
(4) The spatial heterogeneity of sources of brGDGTs on the Berau shelf complicates the use of brGDGTs as temperature proxies. BIT index values are still useful to indicate a predominant continental origin of the OM, although, as seen in many other environments, BIT index values do not linearly correlate with bulk terrestrial organic matter proxies such as $\delta^{13}C_{TOC}$. Application of the global soil calibration to sedimentary mixtures of brGDGTs in the river-influenced area of the shelf results in a severe underestimation of MAT. This is due to the mixed origin of the brGDGTs, which are not only derived from soil erosion but, likely, also from riverine production, as has been observed for other river systems.
(5) Comparison with other shelf systems indicates that in-situ production of brGDGTs in shelf sediments is a widespread phenomenon that is especially pronounced at water depths of ca. 50–300 m. This is probably the case because benthic in-situ production of heterotrophic brGDGT-producing bacteria is fueled by the higher delivery of organic matter to these sediments as the consequence of higher primary productivity in shelf waters and a decreased mineralization due to the relatively short settling times of particles on the shelf.
(6) For palaeoclimatic studies of marine shelf sediments the application of brGDGTs as proxies is severely complicated by the heterogeneity of sources of brGDGTs. Comparison of the brGDGT composition of soils with those of shelf sediments may assist in deciding if sedimentary brGDGTs are predominantly derived from soil erosion. When $\#rings_{tetra} > 0.7$, other sources than soil must also contribute. Plotting the data in a ternary diagram of %tetra, %penta, and %hexa can also assist in assessing the provenance of sedimentary brGDGTs.

ACKNOWLEDGEMENTS

I thank Anchelique Mets, Denise Dorhout, and Alle Tjipke Hoekstra for experimental work, Dr. Kees Booij and Wim Boer for samples, and Dr. Henko de Stigter and Piet van Gaever for ^{210}Pb activity measurements. I am also grateful to Prof. Jess Tierney and Dr. Chun Zhu and Prof. Rich Pancost for providing raw GDGT data for Lake Towuti and the East China Sea shelf, respectively. The associate editor and three anonymous referees are thanked for providing helpful comments on an earlier draft of this paper. This research was funded by the European Research Council under the EU Seventh Framework Programme (FP7/2007-2013)/ERC grant agreement No. 226600. J.S.S.D. also received funding through the Netherlands Earth System Science Centre (NESSC). The fieldwork during which the sediments were obtained was supported by the Netherlands Foundation for the Advancement of Tropical Research (WOTRO) of the Netherlands Organization for Scientific Research (NWO) and by the Royal Dutch Academy of Arts and Sciences (KNAW).

APPENDIX A

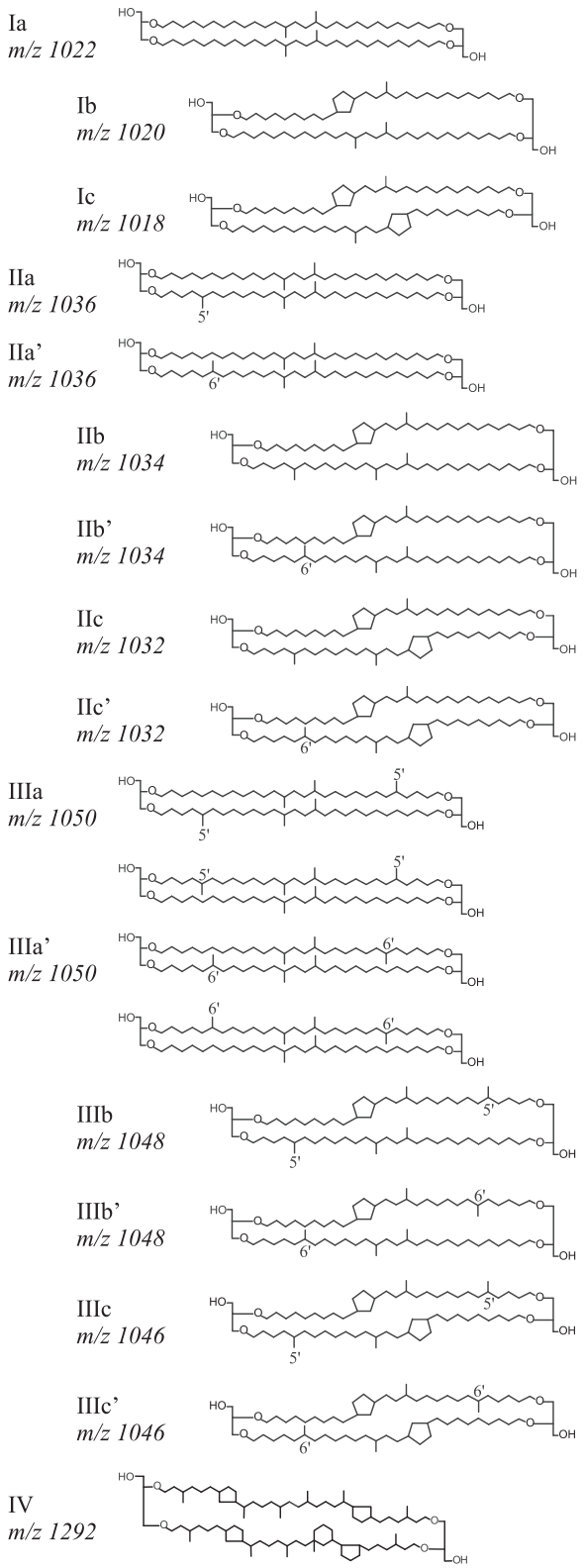

REFERENCES

Bendle J., Weijers J. H. W., Maslin M., Sinninghe Damsté J. S., Schouten S., Hopmans E. C., Boot C. and Pancost R. D. (2010) Major changes in Last Glacial and Holocene terrestrial temperatures and sources of organic carbon recorded in the Amazon fan by the MBT/CBT continental paleothermometer. *Geochem. Geophys. Geosyst.* **11**, Q12007, doi:10.1029/2010GC003308.

Booij K., Arifin Z. and Purbonegoro T. (2012) Perylene dominates the organic contaminant profile in the Berau delta, East Kalimantan, Indonesia. *Mar. Poll. Bull.* **64**, 1049–1054.

Buckles L. K., Weijers J. W. H., Verschuren D. and Sinninghe Damsté J. S. (2014) Sources of core and intact branched tetraether membrane lipids in the lacustrine environment: anatomy of Lake Challa and its catchment, equatorial east Africa. *Geochim. Cosmochim. Acta* **140**, 106–126.

Buschman F. A., Hoitink A. J. F., de Jong S. M., Hoekstra P., Hidayat H. and Sassi M. G. (2012) Suspended sediment load in the tidal zone of an Indonesian river. *Hydrol. Earth Syst. Sci.* **16**, 4191–4204.

Cloern J. E., Canuel E. A. and Harris D. (2002) Stable carbon and nitrogen isotope composition of aquatic and terrestrial plants of the San Francisco Bay estuarine system. *Limnol. Oceanogr.* **47**, 713–729.

De Jonge C., Hopmans E. C., Stadnitskaia A., Rijpstra W. I. C., Hofland R., Tegelaar E. and Sinninghe Damsté J. S. (2013) Identification of novel penta- and hexamethylated branched glycerol dialkyl glycerol tetraethers in peat using HPLC–MS^2, GC–MS and GC–SMB-MS. *Org. Geochem.* **54**, 78–82.

De Jonge C., Hopmans E. C., Zell C. I., Kim J.-H., Schouten S. and Sinninghe Damsté J. S. (2014a) Occurrence and abundance of 6-methyl branched glycerol dialkyl glycerol tetraethers in soils: Implications for palaeoclimate reconstruction. *Geochim. Cosmochim. Acta* **141**, 97–112.

De Jonge C., Stadnitskaia A., Hopmans E. C., Cherkashov G., Fedotov A. and Sinninghe Damsté J. S. (2014b) In situ produced branched glycerol dialkyl glycerol tetraethers in suspended particulate matter from the Yenisei River, Eastern Siberia. *Geochim. Cosmochim. Acta* **125**, 476–491.

De Jonge C., Stadnitskaia A., Hopmans E. C., Cherkashov G., Fedotov A., Streletskaya I. D., Vasiliev A. A. and Sinninghe Damsté J. S. (2015) Drastic changes in the distribution of branched tetraether lipids in suspended matter and sediments from the Yenisei River and Kara Sea (Siberia): implications for the use of brGDGT-based proxies in coastal marine sediments. *Geochim. Cosmochim. Acta* **165**, 200–225.

De Jonge C., Stadnitskaia A., Cherkashov G. and Sinninghe Damsté J. S. (2016) Branched glycerol dialkyl glycerol tetraethers and crenarchaeol record post-glacial sea level rise in the Kara Sea (Arctic Ocean). *Org. Geochem.* **92**, 42–54.

Fietz S., Prahl F. G., Moraleda N. and Rosell-Melé A. (2013) Eolian transport of glycerol dialkyl glycerol tetraethers (GDGTs) off northwest Africa. *Org. Geochem.* **64**, 112–118.

French D. W., Huguet C., Turich C., Wakeham S. G., Carlson L. T. and Ingalls A. E. (2015) Spatial distributions of core and intact glycerol dialkyl glycerol tetraethers (GDGTs) in the Columbia River Basin and Willapa Bay, Washington: insights into origin and implications for the BIT index. *Org. Geochem.* **88**, 91–112.

Hansen J., Ruedy R., Sato M. and Lo K. (2010) Global surface temperature change. *Rev. Geophys.* **48**, RG4004, 10.1029/2010RG000345.

Hopmans E. C., Weijers J. W. H., Schefuß E., Herfort L., Sinninghe Damsté J. S. and Schouten S. (2004) A novel proxy for terrestrial organic matter in sediments based on branched and isoprenoid tetraether lipids. *Earth Planet. Sci. Lett.* **224**, 107–116.

Hopmans E. C., Schouten S. and Sinninghe Damsté J. S. (2016) The effect of improved chromatography on GDGT-based palaeoproxies. *Org. Geochem.* **93**, 1–6.

Huguet C., Hopmans E. C., Febo-Ayala W., Thompson D. H., Sinninghe Damsté J. S. and Schouten S. (2006) An improved method to determine the absolute abundance of glycerol dibiphytanyl glycerol tetraether lipids. *Org. Geochem.* **37**, 1036–1041.

Kim J.-H., Schouten S., Buscail R., Ludwig W., Bonnin J., Sinninghe Damsté J. S. and Bourrin F. (2006) Origin and distribution of terrestrial organic matter in the NW Mediterranean (Gulf of Lions): exploring the newly developed BIT index. *Geochem. Geophys. Geosyst.* **7**. http://dx.doi.org/10.1029/2006GC001306.

Kim J.-H., van der Meer J., Schouten S., Helmke P., Willmott V., Sangiorgi F., Koç N., Hopmans E. C. and Sinninghe Damsté J. S. (2010a) New indices for calibrating the relationship of the distribution of archaeal isoprenoid tetraether lipids with sea surface temperature. *Geochim. Cosmochim. Acta* **74**, 4639–4654.

Kim J.-H., Zarzycka B., Buscail R., Peterse F., Bonnin J., Ludwig W., Schouten S. and Sinninghe Damsté J. S. (2010b) Contribution of river-borne soil organic carbon to the Gulf of Lions (NW Mediterranean). *Limnol. Oceanogr.* **55**, 507–518.

Kim J.-H., Zell C., Moreira-Turcq P., Perez M. A. P., Abril G., Mortillaro J.-M., Weijers J. W. H., Meziane T. and Sinninghe Damsté J. S. (2012) Tracing soil organic carbon in the lower Amazon River and its tributaries using GDGT distributions and bulk organic matter properties. *Geochim. Cosmochim. Acta* **90**, 163–180.

Liu X. L., Zhu C., Wakeham S. G. and Hinrichs K. U. (2014) In situ production of branched glycerol dialkyl glycerol tetraethers in anoxic marine water columns. *Mar. Chem.* **166**, 1–8.

Loh P. S., Chen C. T. A., Lou J. Y., Anshari G. Z., Chen H. Y. and Wang J. T. (2012) Comparing lignin-derived phenols, $\delta^{13}C$ values, OC/N ratio and ^{14}C age between sediments in the Kaoping (Taiwan) and the Kapuas (Kalimantan, Indonesia) rivers. *Aquat. Geochem.* **18**, 141–158.

Loomis S. E., Russell J. M. and Sinninghe Damsté J. S. (2011) Distributions of branched GDGTs in soils and lake sediments from western Uganda: Implications for a lacustrine paleothermometer. *Org. Geochem.* **42**, 739–751.

Loomis S. E., Russell J. M., Ladd B., Street-Perrott F. A. and Sinninghe Damsté J. S. (2012) Calibration and application of the branched GDGT proxy on East African lake sediments. *Earth Planet. Sci. Lett.* **357–358**, 277–288.

Loomis S. E., Russell J. M., Heureux A. M., D'Andrea W. J. and Sinninghé Damsté J. S. (2014) Seasonal variability of branched glycerol dialkyl glycerol tetraethers (brGDGTs) in a temperate lake system. *Geochim. Cosmochim. Acta* **144**, 173–187.

Lü X., Liu X. L., Elling F. J., Yang H., Xie S., Song J., Li X., Yuan H., Li N. and Hinrichs K. U. (2015) Hydroxylated isoprenoid GDGTs in Chinese coastal seas and their potential as a paleotemperature proxy for mid-to-low latitude marginal seas. *Org. Geochem.* **89**, 31–43.

Niemann H., Stadnitskaia A., Wirth S., Gilli A., Anselmetti F. S., Sinninghe Damsté J. S., Schouten S., Hopmans E. C. and Lehmann M. F. (2012) Bacterial GDGTs in Holocene sediments and catchment soils of a high-alpine lake: application of the MBT/CBT-paleothermometer. *Clim. Past* **8**, 889–906.

Oppermann B. I., Michaelis W., Blumenberg M., Frerichs J., Schulz H. M., Schippers A., Beaubien S. E. and Krüger M. (2010) Soil microbial community changes as a result of long-term exposure to a natural CO_2 vent. *Geochim. Cosmochim. Acta* **74**, 2697–2716.

Pancost R. D., Hopmans E. C., Sinninghe Damsté J. S. and the MEDINAUT Shipboard Scientific Party (2001) Archaeal lipids in Mediterranean cold seeps: molecular proxies for anaerobic methane oxidation. *Geochim. Cosmochim. Acta* **65**, 1611–1627.

Pancost R. D. and Sinninghe Damsté J. S. (2003) Carbon isotopic compositions of prokaryotic lipids as tracers of carbon cycling in diverse settings. *Chem. Geol.* **195**, 29–58.

Pearson E. J., Juggins S., Talbot H. M., Weckström J., Rosén P., Ryves D. B., Roberts S. J. and Schmidt R. (2011) A lacustrine GDGT-temperature calibration from the Scandinavian Arctic to Antarctic: renewed potential for the application of GDGT paleothermometry in lakes. *Geochim. Cosmochim. Acta* **75**, 6225–6238.

Peterse F., Kim J.-H., Schouten S., Kristensen D. K., Koc N. and Sinninghe Damsté J. S. (2009a) Constraints on the application of the MBT/CBT palaeothermometer at high latitude environments (Svalbard, Norway). *Org. Geochem.* **40**, 692–699.

Peterse F., Schouten S., van der Meer J., van der Meer M. T. J. and Sinninghe Damsté J. S. (2009b) Distribution of branched tetraether lipids in geothermally heated soils: implications for the MBT/CBT temperature proxy. *Org. Geochem.* **40**, 201–205.

Peterse F., Nicol G. W., Schouten S. and Sinninghe Damsté J. S. (2010) Influence of soil pH on the abundance and distribution of core and intact polar lipid-derived branched GDGTs in soil. *Org. Geochem.* **41**, 1171–1175.

Peterse F., van der Meer J., Schouten S., Weijers J. W. H., Fierer N., Jackson R. B., Kim J.-K. and Sinninghe Damsté J. S. (2012) Revised calibration of the MBT-CBT paleotemperature proxy based on branched tetraether membrane lipids in surface soils. *Geochim. Cosmochim. Acta* **96**, 215–229.

Renema W. (2006) Habitat variables determining the occurrence of large benthic foraminifera in the Berau area (East Kalimantan, Indonesia). *Coral Reefs* **25**, 351–359.

Schmidt F., Hinrichs K. U. and Elvert M. (2010) Sources, transport, and partitioning of organic matter at a highly dynamic continental margin. *Mar. Chem.* **118**, 37–55.

Schoon P. L., de Kluijver A., Middelburg J. J., Downing J. A., Sinninghe Damsté J. S. and Schouten S. (2013) Influence of lake water pH and alkalinity on the distribution of core and intact polar branched glycerol dialkyl glycerol tetraethers (GDGTs) in lakes. *Org. Geochem.* **60**, 72–82.

Schouten S., Huguet C., Hopmans E. C. and Sinninghe Damsté J. S. (2007) Improved analytical methodology of the TEX_{86} paleothermometry by high performance liquid chromatography /atmospheric pressure chemical ionization-mass spectrometry. *Anal. Chem.* **79**, 2940–2944.

Schouten S., Hopmans E. C., Rosell-Melé A., Pearson A., Adam P. and Bauersachs T., et al. (2013a) An interlaboratory study of TEX_{86} and BIT analysis of sediments, extracts, and standard mixtures. *Geochem. Geophys. Geosyst.* **14**, 5263–5285.

Schouten S., Hopmans E. C. and Sinninghe Damsté J. S. (2013b) The organic geochemistry of glycerol dialkyl glycerol tetraether lipids: a review. *Org. Geochem.* **54**, 19–61.

Selver A. D., Sparkes R. B., Bischoff J., Talbot H. M., Gustafsson O., Semiletov I. P., Dudarev O. V., Boult S. and van Dongen B. E. (2015) Distributions of bacterial and archaeal membrane lipids in surface sediments reflect differences in input and loss of terrestrial organic carbon along a cross-shelf Arctic transect. *Org. Geochem.* **83–84**, 16–26.

Sinninghe Damsté J. S., Hopmans E. C., Schouten S., van Duin A. C. T. and Geenevasen J. A. J. (2002) Crenarchaeol: the characteristic core glycerol dibiphytanyl glycerol tetraether

membrane lipid of cosmopolitan pelagic crenarchaeota. *J. Lipid Res.* **43**, 1641–1651.

Sinninghe Damsté J. S., Ossebaar J., Schouten S. and Verschuren D. (2008) Altitudinal shifts in the distribution of branched tetraether lipids in soils from Mt. Kilimanjaro (Tanzania): implications for the MBT/CBT continental palaeothermometer. *Org. Geochem.* **39**, 1072–1076.

Sinninghe Damsté J. S., Ossebaar J., Abbas B., Schouten S. and Verschuren D. (2009) Fluxes and distribution of tetraether lipids in an equatorial African lake: constraints on the application of the TEX_{86} palaeothermometer and BIT index in lacustrine settings. *Geochim. Cosmochim. Acta* **73**, 4232–4249.

Sinninghe Damsté J. S., Rijpstra W. I. C., Hopmans E. C., Weijers J. W. H., Foesel B. U., Overmann J. and Dedysh S. N. (2011) 13,16-Dimethyl octacosanedioic acid (iso-diabolic acid), a common membrane-spanning lipid of Acidobacteria subdivisions 1 and 3. *Appl. Environ. Microbiol.* **77**, 4147–4154.

Sinninghe Damsté J. S., Rijpstra W. I. C., Hopmans E. C., Foesel B., Wüst P., Overmann J., Tank M., Bryant D., Dunfield P., Houghton K. and Stott M. (2014) Ether- and ester-bound iso-diabolic acid and other lipids in Acidobacteria of subdivision 4. *Appl. Environ. Microbiol.* **80**, 5207–5218.

Sparkes R. B., Doğrul Selver A., Bischoff J., Talbot H. M., Gustafsson Ö., Semiletov I. P., Dudarev O. V. and van Dongen B. E. (2015) GDGT distributions on the East Siberian Arctic Shelf: implications for organic carbon export, burial and degradation. *Biogeosciences* **12**, 3753–3768.

Sun Q., Chu G. Q., Liu M. M., Xie M. M., Li S. Q., Ling Y. A., Wang X. H., Shi L. M., Jia G. D. and Lu H. Y. (2011) Distributions and temperature dependence of branched glycerol dialkyl glycerol tetraethers in recent lacustrine sediments from China and Nepal. *J. Geophys. Res.* **116**, G1. http://dx.doi.org/10.1029/2010JG001365.

Tierney J. E. and Russell J. M. (2009) Distributions of branched GDGTs in a tropical lake system: implications for lacustrine application of the MBT/CBT paleoproxy. *Org. Geochem.* **40**, 1032–1036.

Tierney J. E., Russell J. M., Eggermont H., Hopmans E. C., Verschuren D. and Sinninghe Damsté J. S. (2010) Environmental controls on branched tetraether lipid distributions in tropical East African lake sediments. *Geochim. Cosmochim. Acta* **74**, 4902–4918.

Tyson R. V. (1995) *Sedimentary Organic Matter Organic Facies and Palynofacies*, first ed. Chapman & Hall, London, pp. 615.

Walsh E. M., Ingalls A. E. and Keil R. G. (2008) Sources and transport of terrestrial organic matter in Vancouver Island fjords and the Vancouver-Washington margin: a multiproxy approach using delta $\delta^{13}C_{org}$, lignin phenols, and the ether lipid BIT index. *Limnol. Oceanogr.* **53**, 1054–1063.

Weber Y., De Jonge C., Rijpstra W. I. C., Hopmans E. C., Stadnitskaia A., Schubert C. J., Lehmann M. F., Sinninghe Damsté J. S. and Niemann H. (2015) Identification and carbon isotope composition of a novel branched GDGT isomer in lake sediments: evidence for lacustrine brGDGT production? *Geochim. Cosmochim. Acta* **154**, 118–129.

Weijers J. W. H., Schouten S., Spaargaren O. C. and Sinninghe Damsté J. S. (2006) Occurrence and distribution of tetraether membrane in soils: implications for the use of the BIT index and the TEX_{86} SST proxy. *Org. Geochem.* **37**, 1680–1693.

Weijers J. W. H., Schefuss E., Schouten S. and Sinninghe Damsté J. S. (2007a) Coupled thermal and hydrological evolution of tropical Africa over the last deglaciation. *Science* **315**, 1701–1704.

Weijers J. W. H., Schouten S., van den Donker J. C., Hopmans E. C. and Sinninghe Damsté J. S. (2007b) Environmental controls on bacterial tetraether membrane lipid distribution in soils. *Geochim. Cosmochim. Acta* **71**, 703–713.

Weijers J. W. H., Wiesenberg G. L. B., Bol R., Hopmans E. C. and Pancost R. D. (2010) Carbon isotopic composition of branched tetraether membrane lipids in soils suggest a rapid turnover and a heterotrophic life style of their source organism(s). *Biogeosciences* **7**, 2959–2973.

Weijers J. W. H., Schefuβ E., Kim J.-H., Sinninghe Damsté J. S. and Schouten S. (2014) Constraints on the sources of branched tetraether membrane lipids in distal marine sediments. *Org. Geochem.* **72**, 14–22.

Wu W. C., Ruan J. P., Ding S., Zhao L., Xu Y. P., Yang H., Ding W. H. and Pei Y. D. (2014) Source and distribution of glycerol dialkyl glycerol tetraethers along lower yellow river-estuary-coast transect. *Mar. Chem.* **158**, 17–26.

Xie S., Liu X. L., Schubotz F., Wakeham S. G. and Hinrichs K. U. (2014) Distribution of glycerol ether lipids in the oxygen minimum zone of the Eastern Tropical North Pacific Ocean. *Org. Geochem.* **71**, 60–71.

Zell C., Kim J.-H., Lima Sobrinho R., Moreira-Turcq P., Abril G. and Sinninghe Damsté J. S. (2013a) Impact of seasonal hydrological variation on the distributions of isoprenoid and branched tetraether lipids along the Amazon River in the central Amazon basin: Implications for the MBT/CBT paleothermometer. *Front. Microbiol.* **4**, 228.

Zell C., Kim J.-H., Moreira-Turcq P., Abril G., Hopmans E. C., Bonnet M.-P., Lima Sobrinho R. and Sinninghe Damsté J. S. (2013b) Disentangling the origins of branched tetraether lipids and crenarchaeol in the lower Amazon River: Implications for GDGT-based proxies. *Limnol. Oceanogr.* **58**, 343–353.

Zell C., Kim J.-H., Balsinha M., Fernandes C., Dorhout D., Baas M. and Sinninghe Damsté J. S. (2014a) Transport of branched tetraether lipids from the Tagus River basin to the coastal ocean of the Portuguese margin: Consequences for the interpretation of the MBT'/CBT paleothermometer. *Biogeosciences* **11**, 5637–5655.

Zell C., Kim J.-H., Hollander D., Lorenzoni L., Baker P., Silva C., Nittrouer C. and Sinninghe Damsté J. S. (2014b) Sources and distribution of branched and isoprenoid tetraether lipids on the Amazon shelf and fan: Implications for the use of GDGT-based paleothermometers in marine sediments. *Geochim. Cosmochim. Acta* **139**, 293–312.

Zell C., Kim J.-H., Dorhout D., Baas M. and Sinninghe Damsté J. S. (2015) Source and distributions of branched tetraether lipids and crenarchaeol along the Portuguese continental margin: implications for the BIT index. *Cont. Shelf Res.* **96**, 34–44.

Zhu C., Weijers J. W. H., Wagner T., Pan J.-M., Chen J.-F. and Pancost R. D. (2011) Sources and distributions of tetraether lipids in surface sediments across a large river-dominated continental margin. *Org. Geochem.* **42**, 376–386.

Zink K.-G., Vandergoes M. J., Mangelsdorf K., Dieffenbacher Krall A. C. and Schwark L. (2010) Application of bacterial glycerol dialkyl glycerol tetraethers (GDGTs) to develop modern and past temperature estimates from New Zealand lakes. *Org. Geochem.* **41**, 1060–1066.

Associate editor: Elizabeth Ann Canuel